MODELLING THE EFFECTS OF HEPATITIS C VIRUS PLUS-STRAND RNA INFLUX INTO A CELL DURING HEPATITIS C VIRUS REPLICATION

BY

ADAMU ISHAKU
SPS/11/MMT/00002

B.Sc. (Hons.), (G.S.U)

A Dissertation Submitted to the Department of Mathematical Sciences, Bayero University, Kano, in Partial fulfillment of the requirements for the award of the degree of
MASTERS IN MATHEMATICS.

JANUARY, 2016

Declaration

I hereby declare that this work is the product of my research efforts undertaken under the supervision of NAFIU HUSSAINI (PhD) and has not been presented anywhere for the award of a degree or certificate. All sources have been duly acknowledged.

_____

ADAMU ISHAKU

SPS/11/MMT/00002

Certification

This is to certify that the research work for this dissertation and the subsequent write-up were carried out by Adamu Ishaku (SPS/11/MMT/00002) under my supervision.

Dr. Nafiu Hussaini
(Supervisor)

———————————-
Signature

Dr. Bashir Ali
(Head of Department)

———————————-
Signature

Approval

This dissertation has been examined and approved for the award of the degree of MASTERS OF SCIENCE IN MATHEMATICS.

Prof. Babangida Sani ——————————-
(External Examiner) Signature/Date

Dr. Ibrahim Idris ——————————-
(Internal Examiner) Signature/Date

Dr. Nafiu Hussaini ——————————-
(Supervisor) Signature/Date

Dr. Bashir Ali ——————————-
(Head of Department) Signature/Date

——————————- ——————————-
(S.P.S Representative) Signature/Date

Acknowledgment

My first profound gratitude goes to Almighty Allah, for giving me opportunity to complete this project and also the studies. I wish to express my appreciation to my parents Alh. Ishaku Ahmad Kumo, Fatsuma Ishaku, and my step-mother Maryam Ishaku for their moral support.
I wish to express my sincere appreciation to my supervisor Dr. Nafiu Hussaini for his fortitude in giving valuable advice and constant encouragement throughout the period of this research work. Indeed, I am indebted to him for all the corrections made.
I also wish to express my appreciation to my wife Zuwaira Ali Muhammad and my daughter Fatima Adamu Ishaku. I really appreciate your hospitality my aunty Jummai Ahmad, my cousin Dauda Nasiru, and my friends in Kano Kamaluddeen, Abdulrafiq, Ado, and many more.
I appreciate the contributions and generosity of my lecturers Prof. Yahuza Bello, Dr. Ibrahim Idris, Dr. Badakaya, Dr. Bashir Ali, Dr. Maruf Minjibir, Mal. Jamil Hashim, Mal. Hassan, Mal. Mansur, and my colleagues Aliyu Muhd Awwal, Nura M.R. Ahmad, Awwal Bala, Jewaid Rilwan, Munira, Tijjani, and Yahaya Liti.

Dedication

This Research work is dedicated to my daughter Fatima Adamu Ishaku, may Allah Subhanahu Wata'ala bless, guide and protect her.

Table of contents

List of Tables

List of Figures

Abstract

This research work presents a modification of subgenomic Hepatitis C Virus (HCV) replication model in Dahari et al. (2007) by incorporating the rate of influx of HCV plus-strand RNA into Huh-7 cell and monitored its effects. The schematic diagram of HCV replication has been simplified. The model exhibits three equilibria namely trivial equilibrium, healthy equilibrium and endemic equilibrium. Stability analysis of the model shows that the healthy equilibrium is globally asymptotically stable under certain conditions. It has been shown that increase in the rate of influx, increases the steady state level of total plus strand RNA, synthesized plus strand RNA, replicated plus strand RNA and NS5B in the system. Considering this research with the inclusion of receptors that play a role for the entry HCV RNA such as CD81, E2, lipoprotein, SI-BI and bifurcation analysis are recommenced for further research.

CHAPTER ONE

INTRODUCTION

1.1 INTRODUCTION

In this chapter, we give an overview of Hepatitis C Virus infection in section 1.2, significance of our research is in section 1.3, we state the aim and objectives of our research in section 1.5, scope and limitations of this research is discussed in section 1.6, the methodology used in this research work is in section 1.7, and section 1.8 gives the definitions of some basic terms used in this research.

1.2 HEPATITIS C VIRUS INFECTION

Hepatitis C Virus (HCV) is an infectious disease which is very small in size (about 30-60nm in diameter) [32]. It is envelope and belongs to the genus Hepacivirus in the family Flaviviridae [13]. The issue of HCV arose after the development of diagnostic tests for hepatitis A and hepatitis B viruses in the 1970s, when an additional parenterally transmitted agent responsible for majority of transfusions which is not with associated hepatitis A or B was recognized. It was only possible to clone the genome of the virus with the help of recombinant DNA technology, which makes the identification of the virus easier [19]. Since then HCV became a

focus of intense research [6].

The virus affects roughly about 3% of the global population [13, 2]. HCV is often asymptomatic, only in about 15% of the cases. Symptoms include lost of appetite, fatigue, nausea, muscles or joint pain, weight lost, etc.; but chronic infection can cause liver failure and then cirrhosis which can lead to liver transplantation or death [33].

The major means of transmitting HCV is blood-to-blood contact. For instance, blood transfusion, use of poorly sterilized medical equipments, and so on. [28]. The only therapy currently available is combination treatment with a high dose of interferon-α (IFN-α) and the nucleoside analogue ribavirin [31, 20]. Hepatitis c virus replication begins when the virus enters the cell by fusion where the viral genome is released into the cell. The viral genome is then translated by the host ribosome into a viral polyprotein which is cleaved into a core, structural and nonstructural proteins. The viral genome then replicates within the replication vessel by synthesizing a complementary minus-strand RNA using its genome as a template. The newly produced minus-strand RNA is served as a template for the synthesis of a new plus-strand RNA. Eventually, the viral genome participates in assembly and particle formation [33, 13].

1.3 SIGNIFICANCE OF THE STUDY

Understanding HCV replication is one of the major problems in designing new HCV anti-viral agent. Thus, the significance of this research is to gain more useful insights with regard to the dynamics of HCV replication.

1.4 STATEMENT OF THE PROBLEM

We assume that the HCV replication process presented by Dahari et al. [13] is true in vivo, then we incorporate the rate of influx of HCV plus-strand RNA and monitor (mathematically) its effects to production of HCV particles. Further, stability analysis is conspicuously absent in their paper. In this research, we incorporate the rate of influx of HCV plus-strand RNA and compare our result with that of Dahari et al. model in [13] and do some stability analysis.

1.5 AIM AND OBJECTIVES

The main aim of this research work is to investigate the intracellular dynamics of subgenomic HCV RNA replication with rate of influx of HCV plus-strand RNA. The objectives of the research are:

1. To modify the Dahari et al. model in [13].
2. To compute the basic replication number of the modified model.
3. To examine the stability analysis of the equilibria of the modified model.
4. To compare the modified model with the existing Dahari et al. model in [13].

1.6 SCOPE AND LIMITATIONS

HCV replication can be studied either in vitro (i.e technique of performing a giving procedure outside of living organism) or in vivo (i.e technique of performing

a giving procedure within of living organism). This research work models an in vivo study of HCV replication.

Due to lack of experimental data on the number of plus-strands at the time of transfection and the lack of detailed kinetic information about the growth rate of plus-strand RNA, minus-strand RNA and proteins from transfection to steady state, we find it difficult to produce some of Dahari et al. [13] simulation results.

1.7 RESEARCH METHODOLOGY

In our research, we study the HCV life cycle and simplify the schematic diagram used by Dahari et al. in [13] as this helps us to modify Dahari et al. model in [13]. We divide the replication process into three stages: the entry, translation and replication of the virus in our model.

We use reaction kinetics (developed in section 2.3) to formulate the model and simulate the model using computer software MATLAB. The basic replication number is obtained by next generation operator method and we use the basic replication number to find the stability of the model at healthy equilibrium of the modified model. We also simulate the modified model with different values of rate of influx of HCV plus-strand RNA and compare the steady state level of replication mechanisms of Dahari et al. model in [13] and that of the modified model.

1.8 DEFINITION OF BASIC TERMS

Definition 1.8.1 (Infectious Disease) *This is also known as transmitted or communicable disease and it is caused by microscopic germs (such as bacteria or viruses) that get into the body and cause some illness [7].*

Definition 1.8.2 (Cell) *This is the smallest unit of living organism [25].*

Definition 1.8.3 (Huh-7 Cell) *This is a well differentiated hepatocyte derived cellular carcinoma cell that was originally taken from a liver tumor of fifty seven (57) year old Japanese male in 1982. It is the cell line that is used for conducting researches in laboratories [4].*

Definition 1.8.4 (NS5B) *This is the viral RNA dependent RNA polymerase and is the key function of replicating the HCV's viral RNA by using the viral positive strand RNA as its template and catalyzes the polymerization of ribonucleoside triphosphates during RNA replication [13].*

Definition 1.8.5 (Ribosome) *These are tiny particles that are present in large number in all living cells and serve as the site of protein synthesis [22].*

Definition 1.8.6 (Ribonucleic Acid (RNA)) *Is a ubiquitous family of large biological molecules that perform multiple vital roles in the coding, decoding, regulation and expression of genes [26].*

Definition 1.8.7 (Deoxyribonucleic Acid (DNA)) *is a molecule that encodes the genetic instruction used in the development and functioning of all known living organisms and many viruses [26].*

Definition 1.8.8 (Translation) *is a term used in molecular biology and genetics to describe a process in which cellular ribosomes create proteins [34].*

Definition 1.8.9 (Virus Replication) *This is a terminology used by virologists to refer to the formation of biological viruses during infection process in the target host cell [1].*

Definition 1.8.10 (Plus-strand RNA (+sRNA) virus) *It is also known as sense-strand RNA virus whose genetic information consists of a single strand of RNA [26].*

Definition 1.8.11 (Negative-strand RNA (-sRNA) virus) *also known as antisense-strand RNA virus which does not encode mRNA (Messenger RNA) [26].*

Definition 1.8.12 (Genome) *This is simply the complete set of genes in an organism [26].*

Definition 1.8.13 (Subgenomic RNA) *is the messenger for translation of the viral structural proteins and its synthesis that is absolutely required for replication of the virus [26].*

CHAPTER TWO

LITERATURE REVIEW

2.1 INTRODUCTION

This chapter gives an overview of mathematical modelling in Section 2.2 and reaction kinetics in Section 2.3. We also give an updated appraisal of HCV replication models by different researchers including Dahari et al. model published in [13] in Section 2.4 and HCV replication process in section 2.5. Some of the theorems cited in this research are reviewed in 2.6.

2.2 MATHEMATICAL MODELLING

Janak in [36] defined mathematical modeling as the art of using mathematical objects (e.g. differential equations, matrices as well as computer programs) to explain the dynamical or static behaviour of systems/problems we encounter in our day-to-day life .

Some areas of mathematical modelling include:

1. Variuos biological systems (growth, behaviuour, interactions among species, reactions, cellular behaviour and so on).

2. Physical systems (e.g. travelling of light, waves, formation of patterns in nature that we see in animals, universe, atoms, magnetes, motion of planets and so on).

3. Economics (e.g. behaviour of financial market, growth of economies and so on).

4. Social behaviour (e.g. migration, conflicts, interactions and so on).

5. Behaviuor of nature (e.g. formation of earthquakes, tsunamis, clouds, rain, snow, droughts and so on).

6. Industry (e.g. transportation, traffic control/analysis, manufacturing, production lines and so on).

2.2.1 An Algorithm for Modeling

Michael and Gerhard in [18] presented the modeling process as sequence of common steps that serve as an abstraction for the modeler:

1. Identify the problem and questions.

2. Identify the relevant variables in a problem.

3. Simplify until tractable.

4. Relate these variables mathematically.

5. Solve.

6. Does the solution provide added value?

7. Tweak model and compare solutions.

2.3 REACTION KINETICS

Most biochemical reactions are continually taking place in all living organisms and most of them involve proteins called enzymes . In this section, we will discuss the following: Zero order reaction, First order reaction, Second order reaction, and Enzymatic reaction.

2.3.1 Zero Order Reaction

This is the type of reaction that deals with formation (synthesis) or consumption of a certain substance.

For instance, consider the following reaction schemes:

i.

$$A \xrightarrow{k_1} \tag{2.3.1}$$

Consumption of substance A at a constant rate of k_1

ii.

$$\xrightarrow{k_2} B \tag{2.3.2}$$

Formation of substance B at a constant rate of k_2

The rate equations of the reactions schemes (2.3.1) and (2.3.2) are:

i.

$$\frac{dA}{dt} = -k_1 \tag{2.3.3}$$

ii.

$$\frac{dB}{dt} = k_2 \tag{2.3.4}$$

2.3.2 First Order Reaction

In this type of reaction, the product will be formed with respect to reactant or the reactant will be consumed with respect to itself.

For example, consider a substance A producing substance B at a constant rate of k_1 represented by the following reaction scheme:

$$A \xrightarrow{k_1} B \tag{2.3.5}$$

The rate equation for the reaction scheme (2.3.5) is:

$$\frac{dA}{dt} = -k_1 A \tag{2.3.6}$$

$$\frac{dB}{dt} = k_1 A \tag{2.3.7}$$

2.3.3 Second Order Reaction

In this type of reaction, we have two substances A and B reacting to form the product P at a constant rate of k_1, represented by the following reaction scheme:

$$A + B \xrightarrow{k_1} P \tag{2.3.8}$$

The rate equations for the reaction scheme (2.3.8) are:

$$\begin{aligned} \frac{dA}{dt} &= -k_1 AB \\ \frac{dB}{dt} &= -k_1 AB \\ \frac{dP}{dt} &= k_1 AB \end{aligned} \tag{2.3.9}$$

2.3.4 Enzymatic Reaction

One of the essential enzymatic reaction suggested by Michaelis as in [7], involves a substrate S, reacting with enzyme E to form a complex C at a constant rate of k_f and complex C, forms S and E at a constant rate of k_b, the complex C converted into a product P and enzyme E at a constant rate of k_c. The reaction scheme is as follows:

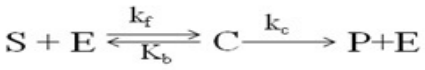

Figure 2.1: *Enzymatic Reaction Scheme*.

The rate equations for the reaction scheme (2.1) are:

$$\begin{aligned} \frac{dS}{dt} &= -k_f SE + k_b C \\ \frac{dE}{dt} &= -k_f SE + k_c C + k_b C \\ \frac{dC}{dt} &= k_f SE - k_b C - k_c C \\ \frac{dP}{dt} &= k_c C \end{aligned} \tag{2.3.10}$$

2.4 HCV REPLICATION MODELS

Hepatitis C Virus is a plus-strand RNA virus which attacks liver cells. HCV replication was studied by different researchers using different methods and the

first study of positive-strand RNA virus replication was done with RNA bacteriophages, (e.g., $Q\beta$ and MS2) by Spiegelman in 1970. Spiegelman showed in [29], that viral RNA amplification depends on an RNA-dependent RNA polymerase-containing RNA replicase that specifically interacts with the incoming viral RNA (plus-strand) to synthesize its complementary minus-strand. Once the minus-strand RNA is synthesized, the amplification of the viral RNA by the replicase begins.

In 1981, Biebricher et al. used the idea developed by Spiegelman in [29] to study the kinetics of RNA amplification by $Q\beta$ replicase (quantitatively) and developed a kinetic model in [17] for self-replication of $Q\beta$ RNA in vitro by Wasley and Alter [3]. The complete life cycle of $Q\beta$ has been mathematically modeled in [24] by Eigen et al. in 1991 which provides a key starting point for developing intracellular HCV replication models.

In 1999, Lohmann et al. designed a bicistronic subgenomic replicon system for HCV in Huh7 cells as published in [34] and since then, it become the standard method for studying HCV replication in a cell. Using a subgenomic genotype 1b (Con1) replicon, Lohmann et al. (1999) found that HCV RNA replication persist in a human hepatoma cell line (Huh-7)1 . Later, the adaptive mutations in non-structural proteins were identified by Bartenschlager et al. [30] which improve the efficiency of HCV replication. However, a full-length HCV genome with these adaptive mutations failed to produce an infectious virus [33].

In 2007, Dahari et al. developed a comprehensive model in [13] for complete

replication of HCV. Considering the biological facts that the translation of the HCV polyprotein takes place in the cytoplasm by involving host ribosomes and the replication of HCV RNA occurs in the vesicular membrane structures (VMS), Dahari et al. tried to address the question "what kind of mechanisms or factors can explain the steady-state observations as published by Quinkert et al. in [8]." The model is based on the HCV replication scheme depicted in Figure 2.2.

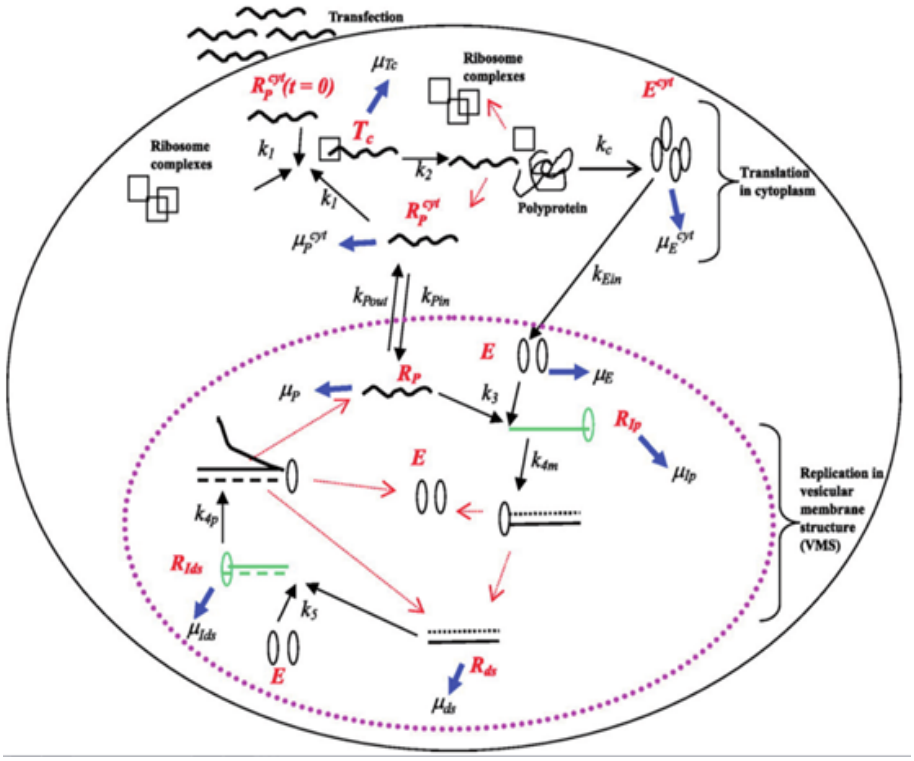

Figure 2.2: *Schematic Diagram Depicted from Dahari et al. Model of HCV Replication Cycle in [13]. The Solid Ellipse Represents Cell Membrane, While Dashed Ellipse Represents the VMS.*

The first four model equations of the following nine equations, explain the translation process and the last five are the equations that describe the replication process.

$$
\begin{aligned}
\frac{dR_p^{cyt}}{dt} &= k_2 T_c + k_{pout} R_p - k_1 R_{ibo} R_p^{cyt} - k_{pin} R_p^{cyt} - \mu_p^{cyt} R_p^{cyt}, \\
\frac{dT_c}{dt} &= k_1 R_{ibo} R_p^{cyt} - k_2 T_c - \mu_{T_c} T_c, \\
\frac{dP}{dt} &= k_2 T_c - k_c P, \\
\frac{dE^{cyt}}{dt} &= k_c P - k_{Ein} E^{cyt} - \mu_E^{cyt} E^{cyt}, \\
\frac{dR_p}{dt} &= k_{4p} R_{Ids} + k_{pin} R_p^{cyt} - k_3 R_p E - k_{pout} R_p - \mu_p R_p, \\
\frac{dR_{ds}}{dt} &= k_{4m} R_{Ip} + k_{4p} R_{Ids} - k_5 R_{ds} E - \mu_{ds} R_{ds}, \\
\frac{dE}{dt} &= k_{Ein} E^{cyt} + k_{4m} R_{Ip} + k_{4p} R_{Ids} - k_3 R_p E - k_5 R_{ds} E - \mu_E E, \\
\frac{dR_{Ip}}{dt} &= k_3 R_p E - k_{4m} R_{Ip} - \mu_{Ip} R_{Ip}, \\
\frac{dR_{Ids}}{dt} &= k_5 R_{ds} E - k_{4p} R_{Ids} - \mu_{Ids} R_{Ids}.
\end{aligned}
\tag{2.4.1}
$$

Statistical technique called meta-analysis was used to assess the clinical effectiveness of healthcare interventions by combining the findings from independent studies of HCV therapeutic vaccination studies in chimpanzees. This was conducted in [12] by Dahari et al. and it revealed that vaccines which contain non-structural HCV proteins were less-effective in curing HCV when compared to inclusion of structural proteins in vaccines which were hypothesized to heighten T-cell response.

Dorner et al. developed a humanized mouse model in [23] using genetic engineering to investigate the viral entry and immunity. Using the model in [23], Dorner et al. showed that human-specific CD81 and occludin plays a role in viral entry into

murine hepatocytes. As a result of using immunocompetent mouse, viral replication and persistence of infection were limited. However, the model was used to study passive immunization.

In 2014, Nikita et al. presented a new stochastic model in [27] for subgenomic HCV replication by considering drug resistant mutants. In [27], Nikita et al. considered the emergence and selection of drug resistant mutant viral RNAs in replicon cells and showed (theoretically) that the observable difference between the viral RNA kinetics for different inhibitors concentration can be explained by differences in the replication rate and inhibitors sensitivity of the mutants RNA.

In this research, we assume that the HCV replication process presented in [13] by Dahari et al. is true in vivo, then we incorporate the rate of influx of HCV plus-strand RNA and monitored (mathematically) its effects to production of more HCV particles.

2.5 HEPATITIS C VIRUS REPLICATION PROCESS

2.5.1 Hepatitis C Virus Entry

Dubuission et al. in [16] found that the virus needs to cross the plasma membrane of the target cell and get access to cytosolic and/or nuclear components in order to replicate its genome. Studies of HCV entry in [5] by Popescu and Dubuission revealed that the process is slow and complex multistep. The viral entry is initiated

by binding of the HCV particle to an attachment factor which helps to concentrate viruses on the cell surface. Ashfaq et al. found that the first step of interaction between HCV and the target cell is required for the initiation of the infection [1]. After binding of the virus to the cell surface, Burlone and Budkowska revealed in [10], that the virus enters the cell by clathrin-dependent endocytosis and upon acidification, fusion of the viral envelope, presumably with the membrane of an early endosome will lead to the release of the viral nucleocapsid into the cytoplasm.

HCV plus- and minus-strand RNA has been estimated in [15] by Ma et al. to be synthesized approximately up to 180nt/min in Huh-7 cells.

The translation and replication processes below are described by Dahari et al. as in [13].

2.5.2 Translation of Hepatitis C Virus RNA

The plus-strand RNA (R_p^{cyp}) enters the cell and then interacts with the host ribosome complex (R_{ibo}) to produce translation complex (T_c) at a constant rate k_1. Once this translation complex is being produced, then translation begins and viral polyprotein (P) will be formed at a constant rate k_2. Thus, T_c degrades at a constant rate of μ_{T_c}. After viral polyprotein is produced, we assume that the ribosome complex dissociate from T_c and that will result to free plus-strand RNA. This R_p^{cyp} degrades at the rate of μ_p^{cyt}. Therefore, R_p^{cyt} and R_{ibo} disappear at a rate of k_1 and then reappear at a rate k_2.

The viral polyprotein alone will then split at a constant rate k_c into separate structural and non-structural viral protein. It is this non-structural viral polyprotein that

include NS5B polymerase (E^{cyt}) which contains RNA replicase which is the replication machinery. Then, E^{cyt} will then degrades with rate constant μ_E^{cyt}. When NS5B is formed, then the translation is complete.

2.5.3 Replication of Hepatitis C Virus RNA

The non-structural viral protein (NS5B polymerase) enters the VMS at a constant rate k_{Ein}. Also, the free plus-strand that dissociate from T_c will also enter the VMS at a constant rate k_{pin}. The free plus-strand in VMS (R_p) will interact with NS5B polymerase in VMS (E) to form plus-strand replicative intermediate complex (R_{Ip}) at a constant rate k_3. The produced R_{Ip} degrades at a rate μ_{Ip}.

The complimentary minus-strand will then be formed at a constant rate of k_{4m} and the R_{Ip} dissociates to double strand RNA (R_{ds}) and NS5B polymerase (E). After the formation of R_{ds}, then E will act on it and leads to the formation of double strand replicative intermediate RNA (R_{Ids}) at a constant rate of k_5 and the formed R_{Ids} degrades at a constant rate of μ_{Ids}. The formed R_{Ids} produces the replicate nascent plus-strand RNA at a constant rate of k_{4p} per complex and once this nascent plus-strand RNA is replicated. The unwounded plus-strand RNA R_p is then released from R_{Ids} complex (along with R_{ds} and E). The replicated plus-strand RNA (R_P) will degrade at a constant rate of μ_p and then transported back to the cytoplasm at a constant rate of k_{pout}. Figure 2.3 represents the diagrammatic explanation of HCV plus-strand RNA entry, translation and replication processes.

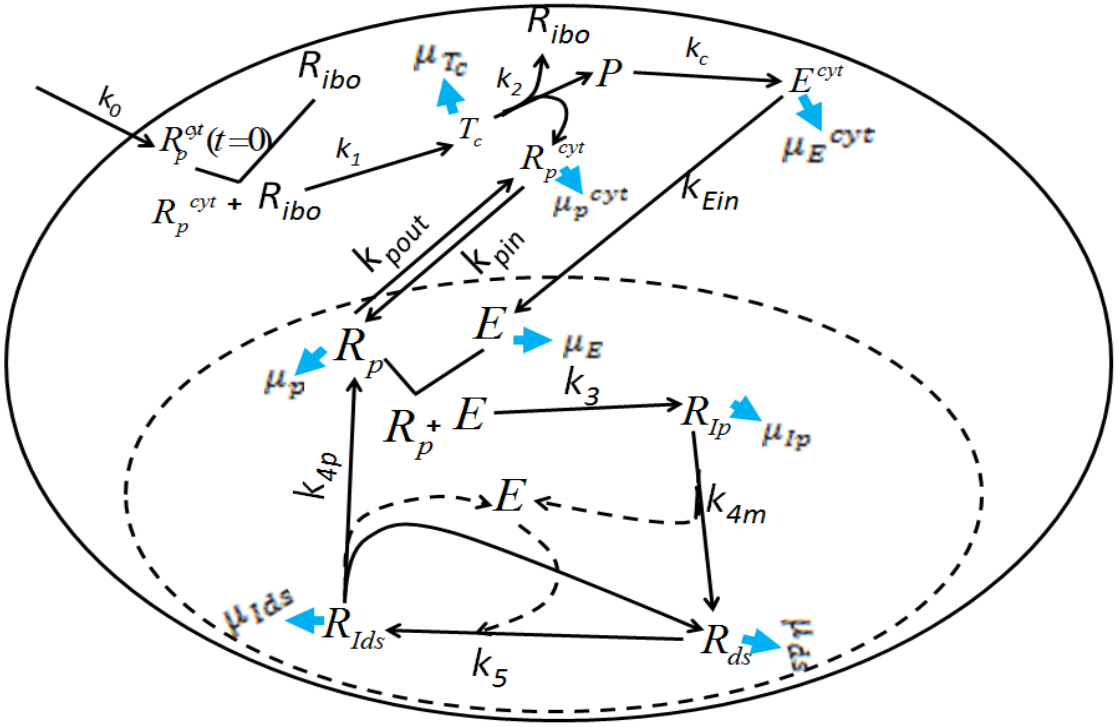

Figure 2.3: *The Reaction Scheme for HCV Replication Process in Huh-7 Cell with k_0 as Rate of Influx of HCV Plus-strand RNA. The Cell Membrane is Symbolised by a Solid Oval Shape and VMS is Symbolised by Dotted Oval Shape.*

2.6 Some of the theorems cited in this research

Consider a disease transmission model with non-negative initial conditions.

$$\begin{aligned} \frac{dx}{dt} &= f(x), \quad x \in \mathbb{R}^n, \quad f : \mathbb{R}^n \to \mathbb{R}^n \\ f &= (f_1, f_2, ..., f_n)^T \\ f_i &= \mathscr{F}_i - \mathscr{V}_i \\ \mathscr{V}_i &= \mathscr{V}_i^- - \mathscr{V}_i^+ \qquad i = 1, 2, .., n. \end{aligned} \tag{2.6.1}$$

$\mathscr{F}_i$ is the rate of appearance of new infection into compartment i,

$\mathscr{V}_i^+$ is the rate of transfer of mechanisms into compartment i,

$\mathscr{V}_i^-$ is the rate of transfer of mechanisms out of compartment i.

Theorem 2.6.1 *[9]*

Consider the disease transmission model 2.6.1 with $f_i(x)$ satisfying conditions (A1) – (A5). If E_1 is a disease free equilibrium of the model, then x_0 is locally asymptotically stable if $R_0 < 1$, but unstable if $R_0 > 1$.

(A1) If $x \geq 0$, then $\mathscr{F}_i, \mathscr{V}_i^+, \mathscr{V}_i^- \geq 0$ for $i = 1, 2, ..., n$.

(A2) If $x = 0$ then $\mathscr{V}_i^- = 0$. In particular, if $x \in X_s = \{x \geq 0 \mid x_i = 0, i = 1, 2, ..., m\}$ which the desease free state then $\mathscr{V}_i^- = 0$ for $i = 1, 2, ..., n$.

(A3) $\mathscr{F}_i = 0$, if $i > m$.

(A4) If $x \in X_s$ then $\mathscr{F}_i(x) = 0$ and $\mathscr{V}_i^+(x) = 0$ for $i = 1, 2, ..., m$.

(A5) If $\mathscr{F}(x) = (\mathscr{F}_1, \mathscr{F}_2, \ldots, \mathscr{F}_n)^T$ is set to zero, then all eigenvalues of $Df(E_1)$ (which is the jacobian matrix of f evaluated at equilibrium point E_1) have negative real parts.

Consider the following initial value problem for autonomous first order system of differential equations in the time independent variable $t \in [0,\infty)$ and dependent variable x:

$$\frac{dx}{dt} = f(x), \qquad x(0) = x_0 \tag{2.6.2}$$

Here $f : \mathbb{R}^m \to \mathbb{R}^m$ and $x, x_0 \in \mathbb{R}^m$ are the given data.

Theorem 2.6.2 *[21]*

Let $\bar{x}$ be an equilibrium point of a dissipative dynamical system on Ω defined by (2.6.2). Let V be a positive definite Lyapunov function for $\bar{x}$ on the set Ω. Furthermore, let $\varepsilon = \{x \in \Omega : \dot{V}(x) = 0\}$. If $M \subset \Omega$, then $\bar{x}$ is globally asymptotically stable on Ω, if and only if it is globally asymptotically stable for the system restricted to M.

Comparison Theorem

The major idea of this theorem is to compare the solutions of the following dynamical system:

$$\frac{dx}{dt} = f(t,x) \tag{2.6.3}$$

with the solution of differential inequality:

$$\frac{dz}{dt} \leq f(t,x), \tag{2.6.4}$$

$$\frac{dy}{dt} \geq f(t,x). \tag{2.6.5}$$

Theorem 2.6.3 *[21]*

Let f be continuous on $\mathbb{R} \times D$, and of type K. Let $x(t)$ be a solution of 2.6.3 defined on [a,b]. If $z(t)$ is a continuous function on [a,b] satisfying 2.6.4 on (a,b), with $z(a) \leq x(a)$, then $z(t) \leq x(t)$ for all t in [a,b]. If $y(t)$ is continuous on [a,b] satisfying 2.6.5 on (a,b), with $y(a) \geq x(a)$, then $y(t) \geq x(t)$ for all $t \in [a,b]$.

CHAPTER THREE

MODEL FORMULATION

3.1 INTRODUCTION

In this chapter, we give different forms of rate equations for each mechanism in Section 3.2 and we derive the modified model equations in Section 3.3 using the techniques of reaction kinetics discussed in section 2.3. The analysis of the model is discussed in Section 3.5.

3.2 RATE EQUATIONS

In order to form the model, we divide the schematic diagram in to sub-units by considering the mechanisms (i.e R_p^{cyt}, T_c, P, E^{cyt}, R_p, E, R_{ds}, R_{Ip}, and R_{Ids}) and express the rate of change of concentration of each mechanism over period of time using technique of reaction kinetics discussed in Section 2.3. The arrow pointing a mechanism represents the formation of that mechanism, the arrow leaving a mechanism represents consumption of that mechanism, and the dotted arrow represents degradation of that mechanism.

3.2.1 Rate equations of plus-strand RNA in the cytoplasm (R_p^{cyt})

Plus-strand RNA in the cytoplasm (R_p^{cyt}) interacts with cell ribosome (R_{ibo}) and form translation complex (T_c) at a constant rate of k_1. After the formation of T_c, (R_p^{cyt}) and R_{ibo} dissociate from T_c at a constant rate of k_2. The dissociated (R_p^{cyt}) enters the VMS at a constant rate of k_{pin} and after the replicated copy is produced, it is transported back to the cytoplasm at a constant rate of k_{pout} an degrades at a constant rate of μ_p^{cyt}. Hence the following figure:

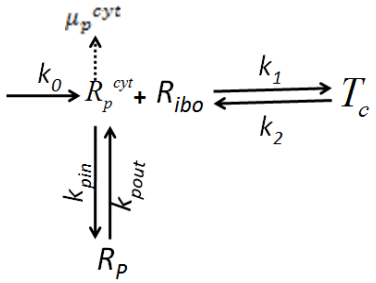

Figure 3.4: *Reaction Scheme for* (R_p^{cyt}) *Extracted from Figure 2.3.*

Rates of formation of R_p^{cyt}: $\dot{u}_{inf} = k_0 R_p^{cyt}$, $\dot{u}_1 = k_2 T_c$, and $\dot{u}_2 = k_{pout} R_p$.
Rates of consumption of R_p^{cyt}: $\dot{u}_3 = k_1 R_{ibo} R_p^{cyt}$ and $\dot{u}_4 = k_{pin} R_p^{cyt}$.
Rates of degradation of R_p^{cyt}: $\dot{u}_5 = \mu_p^{cyt} R_p^{cyt}$.

3.2.2 Rate equations of translation complex (T_c))

Translation complex (T_c) is produced as a result of interaction between plus-strand RNA in the cytoplasm (R_p^{cyt}) and ribosome complex (R_{ibo}). (T_c) degrades at a constant rate of μ^{T_c} and then viral polyprotein (P) will be form from (T_c). Hence the figure 3.5:

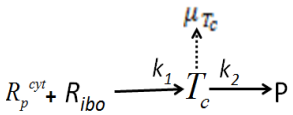

Figure 3.5: *Reaction Scheme for T_c Extracted from Figure 2.3*

Rates of formation of T_c: $\dot{u}_6 = k_1 R_{ibo} R_p^{cyt}$.

Rates of consumption of T_c: $\dot{u}_7 = k_2 T_c$.

Rates of degradation of T_c: $\dot{u}_8 = \mu_{T_c} T_c$.

3.2.3 Rate equations of viral polyprotein (P)

The formed viral polyprotein (P) from translation complex (T_c) at a constant rate of k_2 will produce NS5B polymerase polymerase in the cytoplasm (E^{cyt}). Therefore we have figure 3.6:

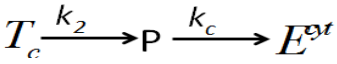

Figure 3.6: *Reaction Scheme for T_c Extracted from Figure 2.3.*

Rates of formation of P: $\dot{u}_9 = k_2 T_c$.

Rates of consumption of P: $\dot{u}_{10} = k_c P$.

No rate of degradation.

3.2.4 Rate equations of NS5B polymerase in the cytoplasm(E^{cyt})

The NS5B polymerase in the cytoplasm(E^{cyt}) that is produced from viral polyprotein (P) at a constant rate of k_c degrades at a constant of μ_E^{cyt}. (E^{cyt}) will produce non-structural NS5B polymerase (E) that enters the cell at a constant rate of k_{Ein}.

The Figure 3.7 is the diagrammatic explanation:

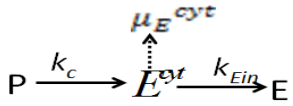

Figure 3.7: *Reaction Scheme for E^{cyt} Obtained Figure 2.3.*

Rates of formation of E^{cyt}: $\dot{u}_{11} = k_c P$.

Rates of consumption of E^{cyt}: $\dot{u}_{12} = k_{Ein} E^{cyt}$.

Rate of degradation of E^{cyt}: $\dot{u}_{13} = \mu_E^{cyt} E^{cyt}$.

3.2.5 Rate equations of plus-strand RNA in VMS (R_p)

The plus-strand RNA in VMS (R_p) is formed at a constant rate of k_{pin} when the dissociated plus-strand RNA in cytoplasm (R_p^{cyt}) and transported back to the cytoplasm at a constant rate of k_{pout}. R_p interact with E to produce plus-strand replicative intermediate (R_{Ip}) at a constant rate of k_3 and degrade at a constant rate of μ_p . Also, double strand RNA replicative intermediate (R_{Ids}) form (R_p). Thus Figure 3.8:

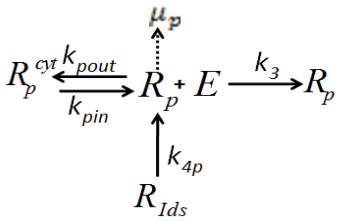

Figure 3.8: *Reaction Scheme for R_p obtained from Figure 2.3*

Rates of formation of R_p: $\dot{u}_{14} = k_{4p} R_{Ids}$, and $\dot{u}_{15} = k_{pin} R_p^{cyt}$.

Rates of consumption of R_p: $\dot{u}_{16} = k_3 R_p E$, and $\dot{u}_{17} = k_{pout} R_p$.

Rate of degradation of R_p : $\dot{u}_{18} = \mu_p R_p$.

3.2.6 Rate equations of NS5B polymerase in VMS (E)

NS5B polymerase in VMS (E) is formed when NS5B polymerase in the cytoplasm (E^{cyt}) splits to structural and non-structural polyprotein including E at a constant rate of k_{Ein}. This E interact with R_p and form R_{Ip} at a constant rate of k_3. E then degrade at a constant rate of μ_E. The formed R_{Ip} produce double strand RNA (R_{ds}) and E at a constant rate of k_{4m}. R_{ds} and E then form double strand RNA replicative intermediate (R_{Ids}) at a constant rate of k_5. R_{Ids} then produce R_{ds}, E, and R_p at a constant rate of k_{4p}. Hence figure 3.9:

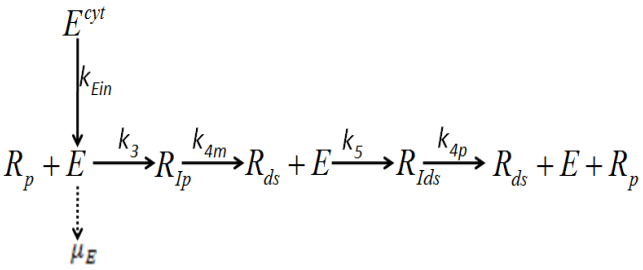

Figure 3.9: *Reaction Scheme for E Obtained from Figure 2.3*

Rates of formation of E: $\dot{u}_{19} = k_{Ein} E^{cyt}$, $\dot{u}_{20} = k_{4m} R_{Ip}$, $\dot{u}_{21} = k_{4p} R_{Ids}$.

Rates of consumption of E: $\dot{u}_{22} = k_3 R_p E$ and $\dot{u}_{23} = k_5 R_{ds} E$.

Rate of degradation of E: $\dot{u}_{24} = \mu_E E$.

3.2.7 Rate equations of double strand RNA (R_{ds})

Plus-strand replicative intermediate (R_{Ip}) form double strand RNA (R_{ds}) and polyprotein (E) at a constant rate of k_{4m}. The formed R_{ds} and E interact and produce double strand RNA replicative intermediate (R_{Ids}) and E at a constant rate of k_5. Also, R_{Ids} formed R_{ds} at a constant rate of k_{4p} and then R_{ds} degrades at a constant rate of μ_{ds}. Hence, Figure 3.10 gives the diagrammatic explanation.

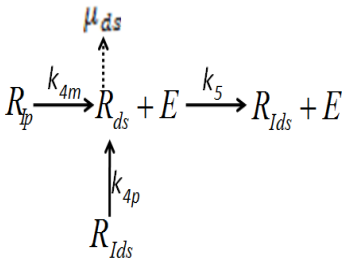

Figure 3.10: *Reaction Scheme for R_{ds} Extracted from Figure 2.3*

Rates of formation of R_{ds}: $\dot{u}_{25} = k_{4m}R_{Ip}$ and $\dot{u}_{26} = k_{4p}R_{Ids}$.

Rates of consumption of R_{ds}: $\dot{u}_{27} = k_5 R_{ds}E$.

Rate of degradation of R_{ds}: $\dot{u}_{28} = \mu_{ds}R_{ds}$.

3.2.8 Rate equations of plus-strand replicative intermediate (R_{Ip})

Plus-strand replicative intermediate (R_{Ip}) is formed as a result of interaction between plus-strand RNA in VMS (R_p) and NS5B polymerase in VMS (E) at a constant rate of k_3 and degrade at a constant rate of μ_{Ip}. The formed R_{Ip} will form double strand RNA (R_{ds}) and (E) at a constant rate of k_{4m}. Hence, Figure 3.11 represents the reaction of R_{ds}.

Rates of formation of R_{Ip}: $\dot{u}_{29} = k_3 R_p E$.

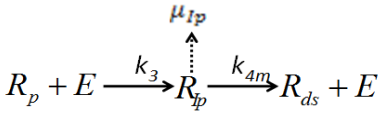

Figure 3.11: *Reaction Scheme for R_{ds} as Obtained from Figure 3.11*

Rates of consumption of R_{Ip}: $\dot{u}_{30} = k_{4m}R_{Ip}$.

Rate of degradation of R_{Ip}: $\dot{u}_{31} = \mu_{Ip}R_{Ip}$.

3.2.9 Rate equations of double-strand replicative intermediate(R_{Ids})

Plus-strand replicative intermediate (R_{Ids}) is obtained when double strand RNA (R_{ds}) interacts with NS5B polymerase in VMS (E) at a constant rate of k_5. R_{Ids} degrades at a constant rate of μ_{Ids}, then plus-strand RNA in VMS (R_p) and NS5B polymerase in VMS (E) were formed at a constant rate of k_{4p}. Hence Figure 3.12 explain the reaction scheme

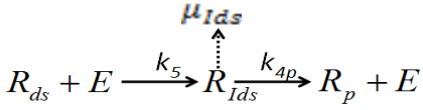

Figure 3.12: *Reaction Scheme for R_{Ids} Extracted from Figure 2.3*

Rates of formation of R_{Ids}: $\dot{u}_{32} = k_5R_{ds}E$.

Rates of consumption of R_{Ids}: $\dot{u}_{33} = k_{4p}R_{Ids}$.

Rate of degradation of R_{Ids}: $\dot{u}_{34} = \mu_{Ids}R_{Ids}$.

3.3 DERIVATION OF THE MODEL EQUATIONS

We use the rate equations developed in Section 3.2 to form the system differential equations using the syntax below:

$$\begin{aligned}\frac{d[\text{mechanism}]}{dt} &= (\text{sum of rates of formation of the mechanism}) \\ &\quad - (\text{sum of rates of consumption of the mechanism}) \\ &\quad - (\text{rate of degradation of the mechanism}).\end{aligned} \tag{3.3.1}$$

The rate of change of concentration of R_p^{cyt} with respect to time is obtained using the syntax 3.3.1 and rate equations in section 3.2.1.

That is:

$$\frac{dR_p^{cyt}}{dt} = (\dot{u}_{inf} + \dot{u}_1 + \dot{u}_2) - (\dot{u}_3 + \dot{u}_4) - \dot{u}_5, \tag{3.3.2}$$

$$\Rightarrow \quad \frac{dR_p^{cyt}}{dt} = k_0 R_p^{cyt} + k_2 T_c + k_{pout} R_p - k_1 R_{ibo} R_p^{cyt} - k_{pin} R_p^{cyt} - \mu_p^{cyt} R_p^{cyt}. \tag{3.3.3}$$

The rate of change of concentration of T_c with respect to time is obtained using the syntax 3.3.1 and rate equations in section 3.2.2.

That is:

$$\frac{dT_c}{dt} = \dot{u}_6 - \dot{u}_7 - \dot{u}_8, \tag{3.3.4}$$

$$\Rightarrow \quad \frac{dT_c}{dt} = k_1 R_{ibo} R_p^{cyt} - k_2 T_c - \mu_{T_c} T_c. \tag{3.3.5}$$

The rate of change of concentration of P with respect to time is obtained using the syntax 3.3.1 and rate equations in section 3.2.3.

Thus,

$$\frac{dP}{dt} = \dot{u}_9 - \dot{u}_{10}, \tag{3.3.6}$$

$$\Rightarrow \quad \frac{dP}{dt} = k_2 T_c - k_c p. \tag{3.3.7}$$

The rate of change of concentration of E^{cyt} with respect to time is obtained using the syntax 3.3.1 and rate equations in section 3.2.4.

Therefore,

$$\frac{dE^{cyt}}{dt} = \dot{u}_{11} - \dot{u}_{12} - \dot{u}_{13}, \tag{3.3.8}$$

$$\Rightarrow \quad \frac{dE^{cyt}}{dt} = k_c P - k_{Ein} E^{cyt} - \mu_E^{cyt} E^{cyt}. \tag{3.3.9}$$

The rate of change of concentration of R_p with respect to time is obtained using the syntax 3.3.1 and rate equations in section 3.2.5.

Thus,

$$\frac{dR_p}{dt} = (\dot{u}_{14} + \dot{u}_{15}) - (\dot{u}_{16} + \dot{u}_{17}) - \dot{u}_{18}, \tag{3.3.10}$$

$$\Rightarrow \quad \frac{dR_p}{dt} = k_{4p} R_{Ids} + k_{pin} R_p^{cyt} - k_3 R_p E - k_{pout} R_p - \mu_p R_p. \tag{3.3.11}$$

The rate of change of concentration of E with respect to time is obtained using the syntax 3.3.1 and rate equations in section 3.2.6.

Thus,

$$\frac{dE}{dt} = (\dot{u}_{19} + \dot{u}_{20} + \dot{u}_{21}) - (\dot{u}_{22} + \dot{u}_{23}) - \dot{u}_{24}, \tag{3.3.12}$$

$$\Rightarrow \quad \frac{dE}{dt} = k_{Ein} E^{cyt} + k_{4m} R_{Ip} + k_{4p} R_{Ids} - k_3 R_p E - k_5 R_{ds} E - \mu_E E. \tag{3.3.13}$$

The rate of change of concentration of R_{ds} with respect to time is obtained using the syntax 3.3.1 and rate equations in section 3.2.7.

Therefore,

$$\frac{dR_{ds}}{dt} = (\dot{u}_{25} + \dot{u}_{26}) - \dot{u}_{27} - \dot{u}_{28}, \tag{3.3.14}$$

$$\Rightarrow \quad \frac{dR_{ds}}{dt} = k_{4m}R_{Ip} + k_{4p}R_{Ids} - k_5R_{ds}E - \mu_{ds}R_{ds}. \tag{3.3.15}$$

The rate of change of concentration of R_{Ip} with respect to time is obtained using the syntax 3.3.1 and rate equations in section 3.2.8.

Thus,

$$\frac{dR_{Ip}}{dt} = \dot{u}_{29} - \dot{u}_{30} - \dot{u}_{31}, \tag{3.3.16}$$

$$\Rightarrow \quad \frac{dR_{Ip}}{dt} = k_3R_pE - k_{4m}R_{Ip} - \mu_{Ip}R_{Ip}. \tag{3.3.17}$$

The rate of change of concentration of R_{Ids} with respect to time is obtained using the syntax 3.3.1 and rate equations in section 3.2.9.

That is:

$$\frac{dR_{Ids}}{dt} = \dot{u}_{32} - \dot{u}_{33} - \dot{u}_{34}, \tag{3.3.18}$$

$$\Rightarrow \quad \frac{dR_{Ids}}{dt} = k_5R_{ds}E - k_{4p}R_{Ids} - \mu_{Ids}R_{Ids}. \tag{3.3.19}$$

3.4 THE MODIFIED DAHARI ET AL. (2007) MODEL

The model 3.4.1 is obtained from (equations 3.3.3 to 3.3.19) and our modified model which differs from that of Dahari et al. [13] by addition of the term $K_0R_p^{cyt}$ (which is the rate of influx of HCV plus-strand RNA) appearing in the first equation of the model 3.4.1.

$$
\begin{aligned}
\frac{dR_p^{cyt}}{dt} &= k_0 R_p^{cyt} + k_2 T_c + k_{pout} R_p - k_1 R_{ibo} R_p^{cyt} - k_{pin} R_p^{cyt} - \mu_p^{cyt} R_p^{cyt}, \\
\frac{dT_c}{dt} &= k_1 R_{ibo} R_p^{cyt} - k_2 T_c - \mu_{T_c} T_c, \\
\frac{dP}{dt} &= k_2 T_c - k_c p, \\
\frac{dE^{cyt}}{dt} &= k_c P - k_{Ein} E^{cyt} - \mu_E^{cyt} E^{cyt}, \\
\frac{dR_p}{dt} &= k_{4p} R_{Ids} + k_{pin} R_p^{cyt} - k_3 R_p E - k_{pout} R_p - \mu_p R_p, \\
\frac{dR_{ds}}{dt} &= k_{4m} R_{Ip} + k_{4p} R_{Ids} - k_5 R_{ds} E - \mu_{ds} R_{ds}, \\
\frac{dE}{dt} &= k_{Ein} E^{cyt} + k_{4m} R_{Ip} + k_{4p} R_{Ids} - k_3 R_p E - k_5 R_{ds} E - \mu_E E, \\
\frac{dR_{Ip}}{dt} &= k_3 R_p E - k_{4m} R_{Ip} - \mu_{Ip} R_{Ip}, \\
\frac{dR_{Ids}}{dt} &= k_5 R_{ds} E - k_{4p} R_{Ids} - \mu_{Ids} R_{Ids}.
\end{aligned}
\tag{3.4.1}
$$

Table 3.1: *Description of Variables in Model 3.4.1.*

Variable	Description
R_p^{cyt}	Plus-strand RNA in cytoplasm
T_c	Translation complex
P	Viral polyprotein
E^{cyt}	NS5B polymerize in cytoplasm
R_p	Plus-strand RNA in VMS
R_{ds}	Double-strand RNA in VMS
E	NS5B polymerize in VMS
R_{Ip}	Plus-strand replicative intermediate
R_{Ids}	Double-strand replicative intermediate

Table 3.2: *Description of Parameters and Parameter Values for Model 3.4.1.*

Parameter	Description	Value	Citation
k_1	Rate constant of T_c formation	80	[13]
k_2	Rate constant of polyprotein translation	100	Assumed
k_3	Rate constant of R_{Ip} formation	0.02	Assumed
k_{4p}	Rate constant of R_P synthesis	1.7	Assumed
k_{4m}	Rate constant of R_{ds} synthesis	1.7	Assumed
k_5	Rate constant of R_{Ids} formation	4 $molecule^{-1}$	[13]
k_{pout}	Rate constant of R_P transport into cytoplasm	0.2	[13]
k_{pin}	Rate constant of R_P^{cyt} transport into VMS	0.2	[13]
k_{Ein}	Rate constant of E^{cyt} transport into VMS	1.3×10^{-5}	[13]
k_c	Rate constant of Viral polyprotein cleavage	0.6	[13]
μ_p^{cyt}	Rate constant of R_P^{cyt} degradation	10	Assumed
μ_p	Rate constant of R_P degradation	0.07	[35]
μ_{ds}	Rate constant of R_{ds} degradation	0.06	[11]
μ_{Ip}	Rate constant of R_{Ip} degradation	0.04	Assumed
μ_{Ids}	Rate constant of R_{Ids} degradation	0.13	[13]
μ_{T_c}	Rate constant of T_c degradation	0.015	Assumed
μ_E	Rate constant of E degradation	0.04	Assumed
μ_E^{cyt}	Rate constant of E^{cyt} degradation	0.06	[11]
$R_P^{Cyp}(0)$	Initial quantity of plus-strand RNA	500	[13]
R_{ibo}^{Tot}	Number of ribosome complex	700	[13]

3.5 ANALYSIS OF THE MODIFIED DAHARI ET AL. (2007) MODEL

The variable in table 3.1 were change to $x_i, i = 1,2,3,...,9$ for easy analysis. Let $R_p^{cyt} = x_1$, $T_c = x_2$, $P = x_3$, $E^{Cyt} = x_4$, $R_p = x_5$, $R_{ds} = x_6$, $E = x_7$, $R_{Ip} = x_8$, and

$R_{Ids} = x_9$ in equation 3.4.1, then we have:

$$\begin{aligned}
\frac{dx_1}{dt} &= k_0 x_1 + k_2 x_2 + k_{pout} x_5 - k_1 R_{ibo} x_1 - k_{pin} x_1 - \mu_p^{cyt} x_1, \\
\frac{dx_2}{dt} &= k_1 R_{ibo} x_1 - k_2 x_2 - \mu_{T_c} x_2, \\
\frac{dx_3}{dt} &= k_2 x_2 - k_c x_3, \\
\frac{dx_4}{dt} &= k_c x_3 - k_{Ein} x_4 - \mu_E^{cyt} x_4, \\
\frac{dx_5}{dt} &= k_{4p} x_9 + k_{pin} x_1 - k_3 x_5 x_7 - k_{pout} x_5 - \mu_p x_5, \\
\frac{dx_6}{dt} &= k_{4m} x_8 + k_{4p} x_9 - k_5 x_6 x_7 - \mu_{ds} x_6, \\
\frac{dx_7}{dt} &= k_{Ein} x_4 + k_{4m} x_8 + k_{4p} x_9 - k_3 x_5 x_7 - k_5 x_6 x_7 - \mu_E x_7, \\
\frac{dx_8}{dt} &= k_3 x_5 x_7 - k_{4m} x_8 - \mu_{Ip} x_8, \\
\frac{dx_9}{dt} &= k_5 x_6 x_7 - k_{4p} x_9 - \mu_{Ids} x_9.
\end{aligned} \tag{3.5.1}$$

3.5.1 Positivity of solution

The model monitors number of molecules of replication mechanism during HCV replication, then we need to show that for non-negative initial conditions, the variables $x_i(t), \quad i = 1,2,\ldots,9$ are positive and remain positive for all $t \geq 0$. Hence the following result.

Lemma 3.5.1 *If $x_i(0) > 0$, for $i = 1,2,...,9$, then the solution $x_i(t)$, for $i = 1,2,\ldots,9$ of the model (3.5.1) are positive for all $t \geq 0$.*

Proof Adopting the prove by contradiction method used in proving the positivity of solution of system of nonlinear equations in [14], we prove this lemma by contradiction.

Suppose there exists a time t_j such that

$$\begin{aligned} x_j(t_j) = 0, \quad x_j'(t_j) < 0, \quad j = 1,2,3,...,9, \\ x_i(t) > 0 \quad i \neq j, \quad i = 1,2,3,...,9, \quad 0 < t < t_j. \end{aligned} \tag{3.5.2}$$

Since the model parameters are positive, then from assumption (3.5.2) and :

first equation in model(3.5.1) (i.e j=1), we have

$$x_1'(t_1) = k_2 x_2 + k_{pout} x_5 > 0, \tag{3.5.3}$$

second equation in model(3.5.1) (i.e j=2) , we have

$$x_2'(t_2) = k_1 R_{ibo} x_1 > 0, \tag{3.5.4}$$

third equation in model (3.5.1) (i.e j=3), we have

$$x_3'(t_3) = k_2 x_2 > 0, \tag{3.5.5}$$

fourth equation in model (3.5.1) (i.e j=4), we have

$$x_4'(t_4) = k_c x_3 > 0, \tag{3.5.6}$$

fifth equation in model (3.5.1) (i.e j=5), we have

$$x_5'(t_5) = k_{4p} x_9 + k_{pin} x_1 > 0, \tag{3.5.7}$$

sixth equation in model (3.5.1) (i.e j=6), we have

$$x_6'(t_6) = k_{4m}x_8 + k_{4p}x_9 > 0, \tag{3.5.8}$$

seventh equation in model (3.5.1) (i.e j=7), we have

$$x_7'(t_7) = k_{Ein}x_4 + k_{4m}x_8 + k_{4p}x_9 > 0, \tag{3.5.9}$$

eighth equation in model (3.5.1) (i.e j=8), we have

$$x_8'(t_8) = k_3x_5x_7 > 0, \tag{3.5.10}$$

ninth equation in model (3.5.1) (i.e j=9), we have

$$x_9'(t_9) = k_5x_6x_7 > 0. \tag{3.5.11}$$

Hence, from equations (3.5.3 to 3.5.11), the solutions of the model (3.5.1), $x_j(t) > 0, \quad j = 1,2,3,4,5,6,7,8,9$ remain positive for $t \geq 0$. ■

3.5.2 Equilibria of the model

An equilibrium point of a dynamical system 3.5.12 represents a stationary condition for the dynamics.

Given the dynamical system

$$\frac{dx}{dt} = f(x), \quad x \in \mathbb{R}^n, \quad f \in \mathbb{R}^n, \tag{3.5.12}$$

where

$$
\begin{aligned}
x &= x(t) \\
&= (x_1(t), x_2(t), ..., x_n(t)), \\
f &= f(x) \\
&= (f_1, f_2, ..., f_n), \\
f_i &= f_i(x_1(t), x_2(t), ..., x_n(t)), \quad i = 1, 2, ..., n.
\end{aligned}
$$

The point $x = E_p$ is an equilibrium point of system 3.5.12 if $f(E_p) = 0$, where

$$
\begin{aligned}
x &= (x_1(t), x_2(t), x_3(t), ..., x_n(t)), \\
E_p &= (x_1^f, x_2^f, x_3^f, ..., x_n^f), \\
0 &= (0, 0, ..., 0).
\end{aligned}
$$

Now, let

$$
\begin{aligned}
f_1(x) &= k_0x_1 + k_2x_2 + k_{pout}x_5 - k_1R_{ibo}x_1 - k_{pin}x_1 - \mu_p^{cyt}x_1,\\
f_2(x) &= k_1R_{ibo}x_1 - k_2x_2 - \mu_{T_c}x_2,\\
f_3(x) &= k_2x_2 - k_cx_3,\\
f_4(x) &= k_cx_3 - k_{Ein}x_4 - \mu_E^{cyt}x_4,\\
f_5(x) &= k_{4p}x_9 + k_{pin}x_1 - k_3x_5x_7 - k_{pout}x_5 - \mu_px_5,\\
f_6(x) &= k_{4m}x_8 + k_{4p}x_9 - k_5x_6x_7 - \mu_{ds}x_6,\\
f_7(x) &= k_{Ein}x_4 + k_{4m}x_8 + k_{4p}x_9 - k_3x_5x_7 - k_5x_6x_7 - \mu_Ex_7,\\
f_8(x) &= k_3x_5x_7 - k_{4m}x_8 - \mu_{Ip}x_8,\\
f_9(x) &= k_5x_6x_7 - k_{4p}x_9 - \mu_{Ids}x_9.
\end{aligned}
\tag{3.5.13}
$$

Representing our modified model 3.5.1 as

$$
\frac{dx}{dt} = f(x), \tag{3.5.14}
$$

$$
\begin{aligned}
\text{where}\quad x &= (x_1,x_2,x_3,x_4,x_5,x_6,x_7,x_8,x_9)^T,\\
f &= (f_1,f_2,f_3,f_4,f_5,f_6,f_7,f_8,f_9)^T,\\
f_i &= f_i(x_1,x_2,x_3,x_4,x_5,x_6,x_7,x_8,x_9), \quad i = 1,2,...,9.
\end{aligned}
$$

then a point $E = (x_1^f, x_2^f, x_3^f, x_4^f, x_5^f, x_6^f, x_7^f, x_8^f, x_9^f)$ is called an equilibrium point of 3.5.1, if $f(E) = 0$.

Now setting the right-hand side of 3.5.1 to zero, we have

$$\begin{aligned}
k_0 x_1^f + k_2 x_2^f + k_{pout} x_5^f - k_1 R_{ibo} x_1^f - k_{pin} x_1^f - \mu_p^{cyt} x_1^f &= 0,\\
k_1 R_{ibo} x_1^f - k_2 x_2^f - \mu_{T_c} x_2^f &= 0,\\
k_2 x_2^f - k_c x_3^f &= 0,\\
k_c x_3^f - k_{Ein} x_4^f - \mu_E^{cyt} x_4^f &= 0,\\
k_{4p} x_9^f + k_{pin} x_1^f - k_3 x_5^f x_7^f - k_{pout} x_5^f - \mu_p x_5^f &= 0,\\
k_{4m} x_8^f + k_{4p} x_9^f - k_5 x_6^f x_7^f - \mu_{ds} x_6^f &= 0,\\
k_{Ein} x_4^f + k_{4m} x_8^f + k_{4p} x_9^f - k_3 x_5^f x_7^f - k_5 x_6^f x_7^f - \mu_E x_7^f &= 0,\\
k_3 x_5^f x_7^f - k_{4m} x_8^f - \mu_{Ip} x_8^f &= 0,\\
k_5 x_6^f x_7^f - k_{4p} x_9^f - \mu_{Ids} x_9^f &= 0.
\end{aligned} \tag{3.5.15}$$

Obviously, at trivial equilibrium $E_0 = (x_1^0, x_2^0, x_3^0, x_4^0, x_5^0, x_6^0, x_7^0, x_8^0, x_9^0)$, $x_1^0 = x_2^0 = \ldots = x_9^0 = 0$, therefore $E_0 = (0,0,0,0,0,0,0,0,0)$.

Consider an equilibrium point $E_1 = (x_1^1, x_2^1, x_3^1, x_4^1, x_5^1, x_6^1, x_7^1, x_8^1, x_9^1)$, when a cell is healthy (plus-strand RNA (which is x_1) is not in the cell and all other mechanisms (except T_c) are not produced and all other parameters are zeros), thus $x_1^1 = x_3^1 = x_4^1 = x_5^1 = x_6^1 = x_7^1 = x_8^1 = x_9^1 = 0$. The number of free ribosome complexes involved in HCV RNA translation is calculated in [13] as $R_{ibo} = R_{ibo}^{Tot} - T_c$, then we say $T_c = R_{ibo}^{Tot} - R_{ibo}$. Let $T_c = \eta$, then $x_2^1 = \eta$ where $\eta = R_{ibo}^{Tot} - R_{ibo}$. Therefore, $E_1 = (0, \eta, 0, 0, 0, 0, 0, 0, 0)$ is another equilibrium point called healthy equilibrium point.

Lastly, let $E_* = (x_1^*, x_2^*, x_3^*, x_4^*, x_5^*, x_6^*, x_7^*, x_8^*, x_9^*)$ be an equilibrium point when every infection mechanism is present, suppose $E_* = (x_1^*, x_2^*, x_3^*, x_4^*, x_5^*, x_6^*, x_7^*, x_8^*, x_9^*)$ is a

solution of 3.5.1 for which every mechanism is present, that is $x_i^* \neq 0, i = 1,2,...,0$. Therefore, we have an endemic equilibrium point $E_* = (x_1^*, x_2^*, x_3^*, x_4^*, x_5^*, x_6^*, x_7^*, x_8^*, x_9^*)$. Therefore, we have the following equilibria:

1. The trivial equilibrium i.e $E_0 = (0,0,0,0,0,0,0,0,0)$
2. The healthy equilibrium i.e $E_1 = (0, \eta, 0,0,0,0,0,0,0)$
   where $\eta = (R_{ibo}^{Tot} - R_{ibo})$.
3. An endemic equilibrium i.e $E^* = (x_1^*, x_2^*, x_3^*, x_4^*, x_5^*, x_6^*, x_7^*, x_8^*, x_9^*)$

3.5.3 Local Stability Analysis

This subsection gives the analysis of local stability of the equilibria of the model (3.5.1). Let $J(E)$ be the Jacobian matrix of the system (3.5.13) at $E = (x_1^f, x_2^f, x_3^f, x_4^f, x_5^f, x_6^f, x_7^f, x_8^f, x_9^f)$ obtained by finding the partial derivatives of $f_i(x), \quad x = (x_1, x_2, x_3, x_4, x_5, x_6, x_7, x_8, x_9)$ with respect to $x_i, i = 1,2,3,...,9$ as the following:

$$J(E) = \begin{pmatrix} \frac{\partial f_1(x)}{\partial x_1} & \frac{\partial f_1(x)}{\partial x_2} & \frac{\partial f_1(x)}{\partial x_3} & \cdots & \frac{\partial f_1(x)}{\partial x_9} \\ \frac{\partial f_2(x)}{\partial x_1} & \frac{\partial f_2(x)}{\partial x_2} & \frac{\partial f_2(x)}{\partial x_3} & \cdots & \frac{\partial f_2(x)}{\partial x_9} \\ \frac{\partial f_3(x)}{\partial x_1} & \frac{\partial f_3(x)}{\partial x_2} & \frac{\partial f_3(x)}{\partial x_3} & \cdots & \frac{\partial f_3(x)}{\partial x_9} \\ \vdots & \vdots & \vdots & \ddots & \vdots \\ \frac{\partial f_9(x)}{\partial x_1} & \frac{\partial f_9(x)}{\partial x_2} & \frac{\partial f_9(x)}{\partial x_3} & \cdots & \frac{\partial f_9(x)}{\partial x_9} \end{pmatrix}_{[x=E]} \tag{3.5.16}$$

Thus,

$$J(E) = \begin{pmatrix} -a_1 & k_2 & 0 & 0 & k_{pout} & 0 & 0 & 0 & 0 \\ b1 & -a_2 & 0 & 0 & 0 & 0 & 0 & 0 & 0 \\ 0 & k_2 & -k_c & 0 & 0 & 0 & 0 & 0 & 0 \\ 0 & 0 & k_c & -a_3 & 0 & 0 & 0 & 0 & 0 \\ k_{pin} & 0 & 0 & 0 & -k_3 x_7^f - a_4 & 0 & -k_3 x_5^f & 0 & k_{4p} \\ 0 & 0 & 0 & 0 & 0 & -b_2 & -k_5 x_6^f & k_{4m} & k_{4p} \\ 0 & 0 & 0 & k_{Ein} & -k_3 x_7^f & -k_5 x_7^f & -b_3 & k_{4m} & k_{4p} \\ 0 & 0 & 0 & 0 & k_3 x_7^f & 0 & k_3 x_5^f & -a_5 & 0 \\ 0 & 0 & 0 & 0 & 0 & k_5 x_7^f & 0 & k_5 x_6^f & -a_6 \end{pmatrix}, \tag{3.5.17}$$

where

$a_1 = k_1(R_{ibo}^{Tot} - x_2^f) + k_{pin} + \mu_p^c - k_0,$

$a_2 = k_2 + \mu_{T_c},$

$a_3 = k_{Ein} + \mu_E^{cyt},$

$a_4 = k_{pout} + \mu_p,$

$a_5 = k_{4m} + \mu_{Ip},$

$a_6 = k_{4p} + \mu_{Ids},$

$b_1 = k_1(R_{ibo}^{Tot} - x_2^f),$

$b_2 = k_5 x_7^f + \mu_{ds},$

$b_3 = k_5 x_6^f + k_3 x_5^f + \mu_E.$

Local Stability of Trivial Equilibrium (E_0)

The Jacobian matrix 3.5.17 at the trivial equilibrium E_0, $J(E_0)$ and given by

$$J(E_0) = \begin{pmatrix} -a_1 & k_2 & 0 & 0 & k_{pout} & 0 & 0 & 0 & 0 \\ k_1 R_{ibo}^{Tot} & -a_2 & 0 & 0 & 0 & 0 & 0 & 0 & 0 \\ 0 & k_2 & -k_c & 0 & 0 & 0 & 0 & 0 & 0 \\ 0 & 0 & k_c & -a_3 & 0 & 0 & 0 & 0 & 0 \\ k_{pin} & 0 & 0 & 0 & -a_4 & 0 & 0 & 0 & k_{4p} \\ 0 & 0 & 0 & 0 & 0 & -\mu_{ds} & 0 & k_{4m} & k_{4p} \\ 0 & 0 & 0 & k_{Ein} & 0 & 0 & -\mu_E & k_{4m} & k_{4p} \\ 0 & 0 & 0 & 0 & 0 & 0 & 0 & -a_5 & 0 \\ 0 & 0 & 0 & 0 & 0 & 0 & 0 & 0 & -a_6 \end{pmatrix}, \tag{3.5.18}$$

where,

$a_1 = k_1 R_{ibo}^{Tot} + k_{pin} + \mu_p^c - k_0,$

$a_2 = k_2 + \mu_{T_c},$

$a_3 = k_{Ein} + \mu_E^{cyt},$

$a_4 = k_{pout} + \mu_p,$

$a_5 = k_{4m} + \mu_{Ip},$

$a_6 = k_{4p} + \mu_{Ids}.$

The characteristic polynimial of the matrix $J(E_0)$ by $\rho(\lambda) = \mid J(E_0) - \lambda I \mid$, where I is an identity matrix of same order with $J(E_0)$ (i.e 9×9). We then solve the

characteristic polynomial using computer software Matlab and obtain the corresponding eigenvalues associated with $J(E_0)$ as:

$\lambda_1 = -a_6,$

$\lambda_2 = -k_c,$

$\lambda_3 = -a_5,$

$\lambda_4 = -a_3,$

$\lambda_5 = -\mu_{ds},$

$\lambda_6 = -\mu_E,$

$\lambda_7 = -\frac{A}{3} + \frac{2^{\frac{2}{3}}Q}{6} + \frac{3^{-1}2^{\frac{1}{3}}(H-B)}{Q},$

$\lambda_8 = -\frac{A}{3} - (\frac{2^{\frac{2}{3}}Q}{12} + \frac{3^{-1}2^{\frac{1}{3}}(H-B)}{2Q}) - (\frac{2^{\frac{2}{3}}3^{\frac{1}{2}}Q}{12} - \frac{3^{-1}2^{\frac{1}{3}}(H-B)}{2Q})i,$

$\lambda_9 = -\frac{A}{3} - (\frac{2^{\frac{2}{3}}Q}{12} + \frac{3^{-1}2^{\frac{1}{3}}(H-B)}{2Q}) + (\frac{2^{\frac{2}{3}}3^{\frac{1}{2}}Q}{12} - \frac{3^{-1}2^{\frac{1}{3}}(H-B)}{2Q})i,$

where

$A = a_1 + a_2 + a_4,$

$B = a_1a_2 + a_1a_4 + a_2a_4,$

$C = 27a_1a_2a_4,$

$D = 27(a_4k_1k_2R_{ibo}^{Tot} + a_2k_{pin}k_{pout}),$

$E = (k_1k_2R_{ibo}^{Tot} + k_{pin}k_{pout}),$

$F = a_1^2 + a_2^2 + a_4^2,$

$G = (9A(B-E) - 2A^3 - C + D),$

$H = F + 3E,$

$Q = (G + (G^2 - 4(H-B)^3)^{\frac{1}{2}})^{\frac{1}{3}}.$

The following lemma summarise the condition for local stability analysis of trivial equilibruim point (E_0).

Lemma 3.5.2 *Assuming $Q > 0$ then,*

i. E_0 is locally asymptotically stable when $A > (2^{-\frac{1}{3}}Q + 2^{\frac{1}{3}}Q^{-1}(H-B))$.

ii. E_0 is a saddle point when $A < (2^{-\frac{1}{3}}Q + 2^{\frac{1}{3}}Q^{-1}(H-B))$.

Proof Suppose $Q > 0$, then:

i. λ_8 and λ_9 will have negative real parts. Also, since a_3, a_5, a_6, k_c, μ_E, and μ_{ds} are real and positive, then the eigenvalues λ_i , $i = 1,2,3,...,6$ are negative real eigenvalues.

Lastly, λ_7 will be negative when $A > (2^{-\frac{1}{3}}Q + 2^{\frac{1}{3}}Q^{-1}(H-B))$. Thus, λ_i,$i = 1,2,3,4,5,6,7,8,9$ have negative real parts, hence E_0 is locally asymptotically stable.

ii. Since a_3, a_5, a_6, k_c, μ_E, and μ_{ds} are real and positive parameters, then the eigenvalues λ_i , $i = 1,2,3,...,6$ are negative real eigenvalues. Now if $A < (2^{-\frac{1}{3}}Q + 2^{\frac{1}{3}}Q^{-1}(H-B))$, then eigenvalue λ_7 will be positive and λ_8 and λ_9 will have negative real parts. Hence E_0 is a saddle point. ■

Observe that, decreasing the rate of influx of HCV plus-strand RNA (k_0) also increases the value of A which leads to local stability of trivial equilibrium.

Local Stability of Healthy Equilibrium (E_1)

Using next generation method, we compute the basic replication number R_0, which is the threshold parameter that measures the average number of new replicated copies generated by single virus when introduced in to a healthy cell over its entire period. In order to compute R_0, we regard the model (3.5.1) as epidemiological model with nine compartments $x_1, x_2, x_3, x_4, x_5, x_6, x_7, x_8$, and x_9.

The infected compartments are x_1, x_2, and x_5. The infection begins when x_2 was formed, then the rate of formation of x_2 ($k_1 R_{ibo} x_2$) is the force of infection also called new infection term.

Writing system 3.5.1 in the form:

$$\begin{aligned} \frac{dx}{dt} &= \mathscr{F}(x) - \mathscr{V}(x), \\ \mathscr{V}(x) &= \mathscr{V}^-(x) - \mathscr{V}^+(x), \\ x &= (x_1, x_2, x_3, x_4, x_5, x_6, x_7, x_8, x_9)^T, \end{aligned} \tag{3.5.19}$$

where $\mathscr{F}, \mathscr{V}^+, \mathscr{V}^- : \mathbf{R}^9 \to \mathbf{R}^9$,

$\mathscr{F}_i$ is the rate of appearance of new infection into compartment i,

$\mathscr{V}_i^+$ is the rate of transfer of mechanisms into compartment i,

$\mathscr{V}_i^-$ is the rate of transfer of mechanisms out of compartment i,

$$\mathscr{F}(x) = \begin{pmatrix} \mathscr{F}_1(x) \\ \mathscr{F}_2(x) \\ \mathscr{F}_3(x) \\ \mathscr{F}_4(x) \\ \mathscr{F}_5(x) \\ \mathscr{F}_6(x) \\ \mathscr{F}_7(x) \\ \mathscr{F}_8(x) \\ \mathscr{F}_9(x) \end{pmatrix} = \begin{pmatrix} 0 \\ k_1 R_{ibo} x_1 \\ 0 \\ 0 \\ 0 \\ 0 \\ 0 \\ 0 \\ 0 \end{pmatrix}, \quad \mathscr{V}^+(x) = \begin{pmatrix} \mathscr{V}_1^+(x) \\ \mathscr{V}_2^+(x) \\ \mathscr{V}_3^+(x) \\ \mathscr{V}_4^+(x) \\ \mathscr{V}_5^+(x) \\ \mathscr{V}_6^+(x) \\ \mathscr{V}_7^+(x) \\ \mathscr{V}_8^+(x) \\ \mathscr{V}_9^+(x) \end{pmatrix} = \begin{pmatrix} k_0 x_1 + k_2 x_2 + k_{pout} x_5 \\ 0 \\ k_2 x_2 \\ k_c x_3 \\ k_{4p} x_9 + k_{pin} x_1 \\ k_{4m} x_8 + k_{4p} x_9 \\ k_{Ein} x_4 + k_{4m} x_8 + k_{4p} x_9 \\ k_3 x_5 x_7 \\ k_5 x_6 x_7 \end{pmatrix},$$

$$\mathscr{V}^{-}(x) = \begin{pmatrix} \mathscr{V}_1^{-}(x) \\ \mathscr{V}_2^{-}(x) \\ \mathscr{V}_3^{-}(x) \\ \mathscr{V}_4^{-}(x) \\ \mathscr{V}_5^{-}(x) \\ \mathscr{V}_6^{-}(x) \\ \mathscr{V}_7^{-}(x) \\ \mathscr{V}_8^{-}(x) \\ \mathscr{V}_9^{-}(x) \end{pmatrix} = \begin{pmatrix} k_1 R_{ibo} x_1 + k_{pin} x_1 + \mu_p^{cyt} x_1 \\ k_2 x_2 + \mu_{T_c} x_2 \\ k_c x_3 \\ k_{Ein} x_4 + \mu_E^{cyt} x_4 \\ k_3 x_5 x_7 + k_{pout} x_5 + \mu_p x_5 \\ k_5 x_6 x_7 + \mu_{ds} x_6 \\ k_3 x_5 x_7 + k_5 x_6 x_7 + \mu_E x_7 \\ k_{4m} x_8 + \mu_{Ip} x_8 \\ k_{4p} x_9 + \mu_{Ids} x_9 \end{pmatrix}.$$

The infected compartments are x_1, x_2, and x_5, then the associated matrix F for new infection terms is obtained by

$$F = \begin{pmatrix} \frac{\partial \mathscr{F}_1(x)}{\partial x_1} & \frac{\partial \mathscr{F}_1(x)}{\partial x_2} & \frac{\partial \mathscr{F}_1(x)}{\partial x_5} \\ \frac{\partial \mathscr{F}_2(x)}{\partial x_1} & \frac{\partial \mathscr{F}_2(x)}{\partial x_2} & \frac{\partial \mathscr{F}_2(x)}{\partial x_5} \\ \frac{\partial \mathscr{F}_5(x)}{\partial x_1} & \frac{\partial \mathscr{F}_5(x)}{\partial x_2} & \frac{\partial \mathscr{F}_5(x)}{\partial x_5} \end{pmatrix}_{[x=E_1]}.$$

This implies,

$$F = \begin{pmatrix} 0 & 0 & 0 \\ k_1 R_{ibo} & 0 & 0 \\ 0 & 0 & 0 \end{pmatrix}.$$

The associated matrix V for the remaining terms is obtained by

$$V = \begin{pmatrix} \frac{\partial \mathscr{V}_1(x)}{\partial x_1} & \frac{\partial \mathscr{V}_1(x)}{\partial x_2} & \frac{\partial \mathscr{V}_1(x)}{\partial x_5} \\ \frac{\partial \mathscr{V}_2(x)}{\partial x_1} & \frac{\partial \mathscr{V}_2(x)}{\partial x_2} & \frac{\partial \mathscr{V}_2(x)}{\partial x_5} \\ \frac{\partial \mathscr{V}_5(x)}{\partial x_1} & \frac{\partial \mathscr{V}_5(x)}{\partial x_2} & \frac{\partial \mathscr{V}_5(x)}{\partial x_5} \end{pmatrix}_{[x=E_1]}.$$

This implies,

$$V = \begin{pmatrix} k_{pin} + \mu_p^{cyt} + k_1 R_{ibo} - k_0 & -k_2 & -k_{pout} \\ 0 & k_2 + \mu_{Tc} & 0 \\ -k_{pin} & 0 & k_{pout} + \mu_p \end{pmatrix}.$$

Thus, V is a non-singular matrix as required, so we find its inverse. Let τ be the determinant of V, (i.e τ =det(V)) then

$\tau = (k_2 + \mu_{Tc})[k_{pin}\mu_p + (\mu_p^c + k_1 R_{ibo})(k_{pout} + \mu_p) - (k_{pout} + \mu_p)k_0)]$.

Therefore,

$$V^{-1} = \begin{pmatrix} \frac{(k_2+\mu_{Tc})(k_{pout}+\mu_p)}{\tau} & \frac{k_2(k_{pout}+\mu_p)}{\tau} & \frac{k_{pout}(k_2+\mu_{Tc})}{\tau} \\ 0 & \frac{(k_{pin}+\mu_p^{cyt}+k_1R_{ibo}-k_0)(k_{pout}+\mu_p)-k_2k_{pin}}{\tau} & 0 \\ \frac{k_{pin}(k_2+\mu_{Tc})}{\tau} & \frac{-k_{pin}k_2}{\tau} & \frac{(k_{pin}+\mu_p^{cyt}+k_1R_{ibo}-k_0)(k_2+\mu_{Tc})}{\tau} \end{pmatrix}.$$

and

$$FV^{-1} = \begin{pmatrix} 0 & 0 & 0 \\ \frac{k_1R_{ibo}(k_2+\mu_{Tc})(k_{pout}+\mu_p)}{\tau} & \frac{k_1R_{ibo}k_2(k_{pout}+\mu_p)}{\tau} & \frac{k_1R_{ibo}k_{pout}(k_2+\mu_{Tc})}{\tau} \\ 0 & 0 & 0 \end{pmatrix}. \tag{3.5.20}$$

The eigenvalues $\lambda_i, i = 1,2,3$ are obtained by finding the solutions of

$| FV^{-1} - \lambda I | = 0$, where I is an identity matrix of same order with FV^{-1} (i.e 3x3).

This implies,

$$\lambda(\lambda(\frac{k_1R_{ibo}k_2(k_{pout}+\mu_p)}{\tau} - \lambda)) = 0.$$

Thus, the eigenvalues of FV^{-1} are $\lambda_{1,2} = 0$ and $\lambda_3 = \frac{k_1 R_{ibo} k_2 (k_{pout} + \mu_p)}{\tau}$.

Let the spectral radius of the matrix FV^{-1} be defined by $\rho(FV^{-1})$. Mathematically,

$$\rho(FV^{-1}) = max\{\mid \lambda_i \mid, \quad \lambda_i \text{is an eigenvalue of} \quad FV^{-1}\} \tag{3.5.21}$$

Hence,

$$\begin{aligned} R_0 &= \rho(FV^{-1}) \\ &= \frac{k_2 k_1 R_{ibo}(k_{pout} + \mu_p)}{(k_2 + \mu_{Tc})[k_{pin}\mu_p + (\mu_p^c + k_1 R_{ibo})(k_{pout} + \mu_p) - (k_{pout} + \mu_p)k_0)]} \end{aligned} \tag{3.5.22}$$

where ρ is called the spectral radius and $k_0 \geq 0$.

Lemma 3.5.3 *R_0 exists iff $k_0 < \frac{k_{pout}\mu_p}{k_{pout}+\mu_p} + (\mu_p^c + k_1 R_{ibo})$.*

Observe that, increasing the rate of influx of HCV plus-strand RNA (k_0) also increases the value of R_0 which measures the average number of new replicated copies generated by single virus when introduced in to a healthy cell over its entire period. Likewise decreasing k_0 decreases the value of R_0.

express as $R_0 = \frac{k2b_1a_4}{a_2(a_4a_1 - k_{pin}k_{pout})}$. Applying Theorem 2.6.2, the following result is established.

Lemma 3.5.4 *The healthy equilibrium E_1 of the system (3.5.1) is locally asymptotically stable if $R_0 < 1$, and unstable if $R_0 > 1$.*

Biologically speaking, Lemma (3.5.4) implies that the replication can be controlled when $R_0 < 1$, depending on the intial sizes of replication mechanisms in the model (3.5.1).

Stability of healthy equilibrium depends on R_0 and since increasing k_0 increases R_0 and also decreasing k_0 decreases R_0. Hence, increasing k_0 reduces the chance of local stability of healthy equilibrium.

Threshold Analysis

In order to assess the impact of k_0, we differentiate R_0 partially with respect to k_0, since $R_0 = R_0(k_0, k_1, k_2, k_{pin}, k_{pout}, R_{ibo}, \mu_p, \mu_p^{cyt}, \mu_{Tc})$.

Thus, we have:

$$\frac{\partial R_0}{\partial k_0} = \frac{(k_{pout}+\mu_p)^2 k_2 k_1 R_{ibo}}{(k_2+\mu_{Tc})[k_{pout}\mu_p + (\mu_p^{cyt}+k_1 R_{ibo})(k_{pout}+\mu_p) - (k_{pout}+\mu_p)k_0]^2} \tag{3.5.23}$$

Since all the model parameters are non-negative, then $\frac{\partial R_0}{\partial k_0} > 0$, thus the following result.

Lemma 3.5.5 *The rate of influx of HCV plus-strand RNA into Huh-7 cell has detrimental impact in the system.*

Global Stability of Healthy Equilibrium

Lemma 3.5.6 *For system (3.5.1) , the healthy equilibrium E_1 is globally asymptotically stable if $R_0 < 1$ and $k_3 x_5^1 x_7^1 - k_{4p} x_9^1 \geq 0$.*

Proof We use the comparison theorem 2.6.3 to prove the global stability of the healthy equilibrium E_1. The rate of change of the variables x_1, x_2, and x_5 of system

3.5.1 can be rewritten as:

$$\begin{pmatrix} \frac{dx_1}{dt} \\ \frac{dx_2}{dt} \\ \frac{dx_5}{dt} \end{pmatrix} = (F-V) \begin{pmatrix} x_1 \\ x_2 \\ x_5 \end{pmatrix} - \begin{pmatrix} 0 \\ 0 \\ k_3 x_5 x_7 - k_{4p} x_9 \end{pmatrix}$$

where F and V are as defined in Section 3.2. By positivity of solutions and system parameters for all $t \geq 0$, then

$$\begin{pmatrix} \frac{dx_1}{dt} \\ \frac{dx_2}{dt} \\ \frac{dx_5}{dt} \end{pmatrix} \leq (F-V) \begin{pmatrix} x_1 \\ x_2 \\ x_5 \end{pmatrix}$$

Whenever $k_3 x_5^1 x_7^1 - k_{4p} x_9^1 \geq 0$. By lemma 1 of [9] the eigenvalues of the matrix F - V all have negative real parts. Thus, the system 3.5.1 is stable whenever $R_0 < 1$. Therefore,$(x_1, x_2, x_5) \to (0, \eta, 0)$ as $t \to \infty$. By theorem 2.6.1, it follows that $(x_1, x_2, x_5) \to (0, \eta, 0)$ and $(x_3, x_4, x_6, x_7, x_8, x_9) \to (0,0,0,0,0,0)$ as $t \to \infty$. Then $(x_1, x_2, x_3, x_4, x_5, x_6, x_7, x_8, x_9) \to E_1$ as $t \to \infty$. Hence, E_1 is globally asymptotically stable provided $R_0 < 1$. ■

CHAPTER FOUR

RESULTS AND DISCUSSION

4.1 INTRODUCTION

In this chapter, we simulate the modified model in Section 4.2 and we also give the comparative analysis between the existing and modified models in Section 4.3. The detailed explanation of the findings of this research work is discussed in section 4.4.

4.2 NUMERICAL SIMULATIONS

To illustrate the effect of plus-strand RNA in the model (3.5.1), we present the simulations of the model (3.5.1) using the parameter values in table 3.2. We have computed the solution of our modified model numerically using a function ode15s which uses Resenbrock algorithm implemented in in MATLAB R2010a version 7.10.0.499 (see Appendix). We use the fact from Dahari et al. [13] that at the time of transfection (i.e $t = 0$), $x_1(0) = 500$ and $x_i(0) = 0 \quad for \quad i = 2,3,4,5,6,7,8,9$. The total plus-strand RNA in the system is $(x_1 + x_2 + x_5 + x_6 + x_8 + x_9)$, synthesized plus-strand RNA in the cytoplasm (x_1), replicated plus-strand RNA in VMS

(x_5) , and NS5B (x_7). The modified model (3.5.1) was simulated with different values of rate of influx of HCV plus-strand RNA (k_0) and the numerical results are shown in figure (4.13-4.16).

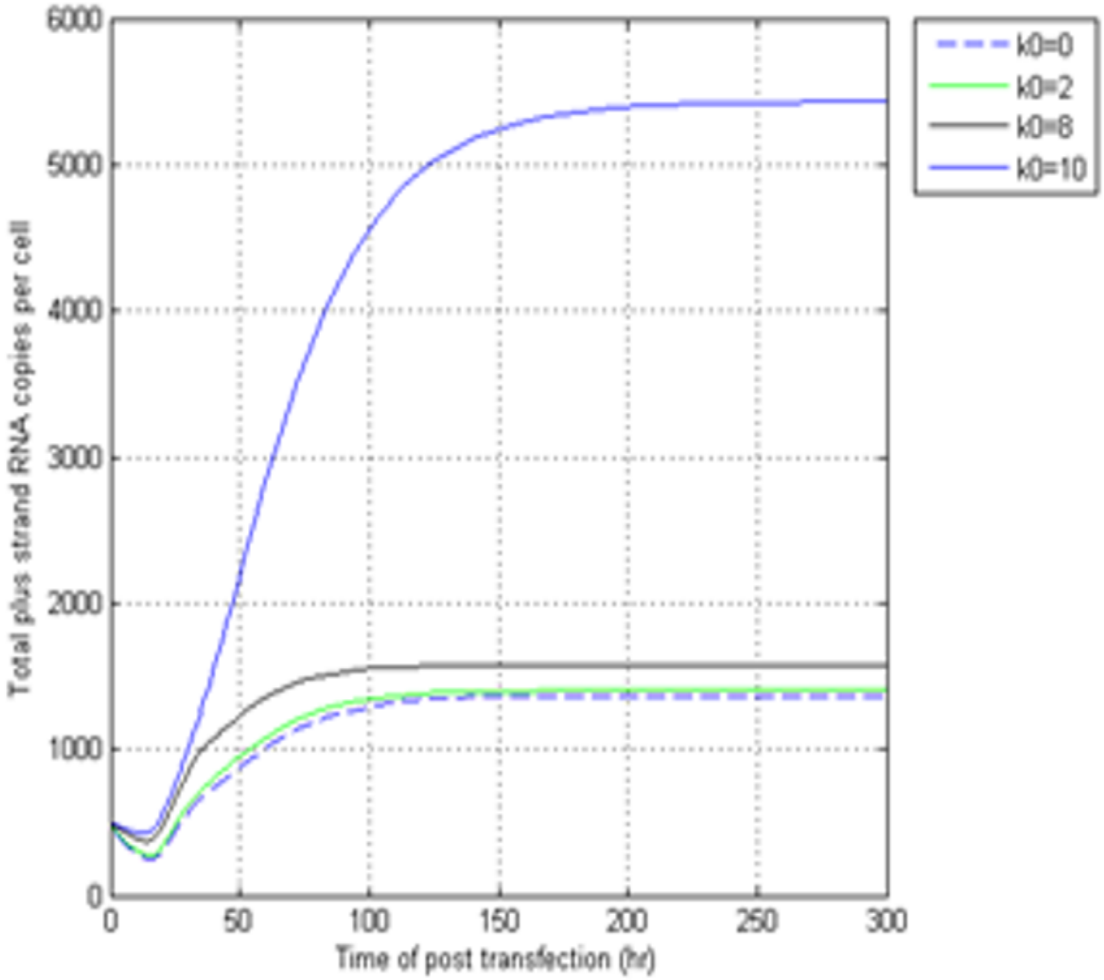

Figure 4.13: *Simulation Results of Model (3.5.1) Showing the Disparity in Steady State Level of Total Plus-strand RNA in the System Caused by Changing Rate of Influx of HCV Plus-strand RNA from* $k_0 = 0$ *Represented by Dashed Blue Line, to* $k_0 = 2$ *Represented by Green Line, to* $k_0 = 8$ *Represented by Black Line, and to* $k_0 = 10$ *Represented by Thick Blue Line.*

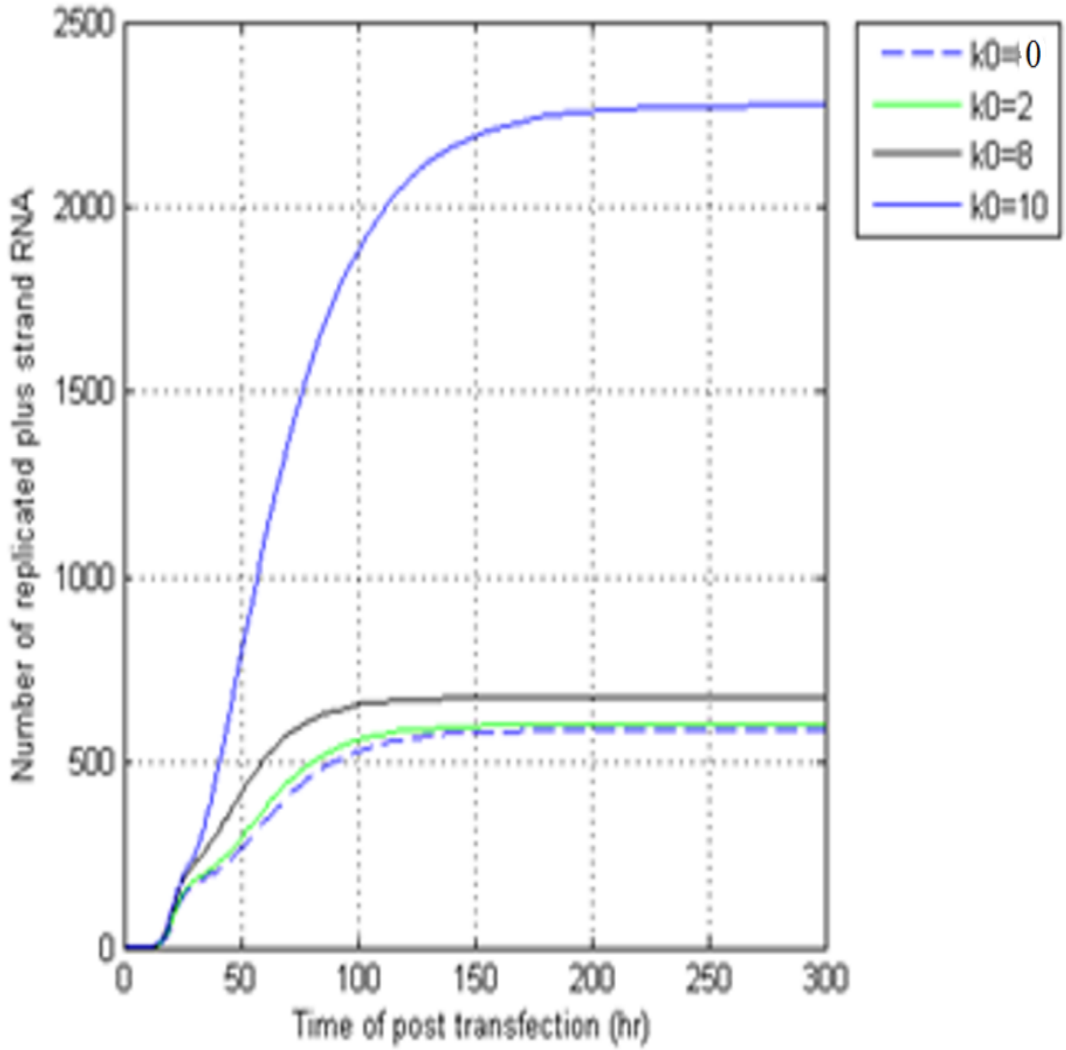

Figure 4.14: *Simulation Results of Model (3.5.1) Showing the Disparity in Steady State Level of Synthesized plus-strand RNA in the cytoplasm Caused by Changing Rate of Influx of HCV Plus-strand RNA from* $k_0 = 0$ *Represented by Dashed Blue Line, to* $k_0 = 2$ *Represented by Green Line, to* $k_0 = 8$ *Represented by Black Line, and to* $k_0 = 10$ *Represented by Thick Blue Line.*

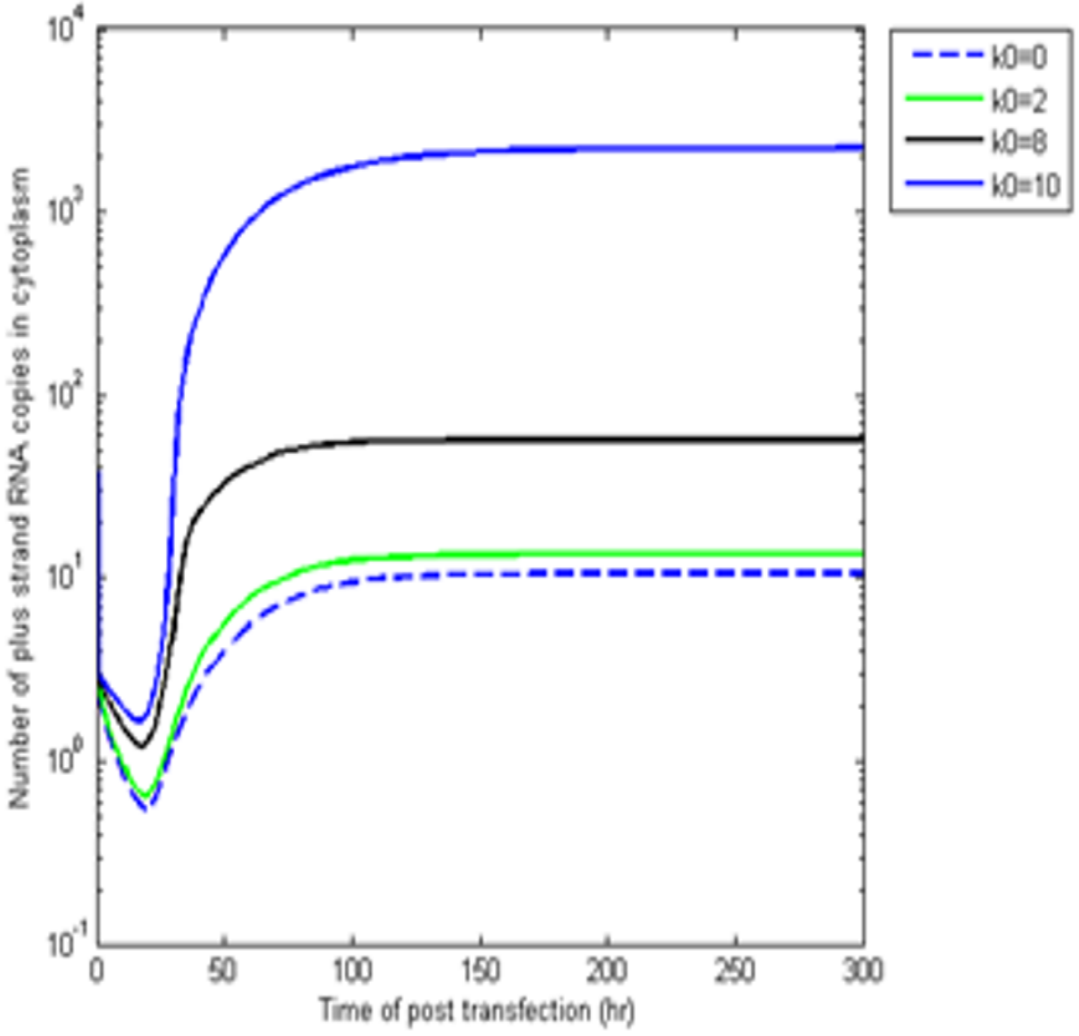

Figure 4.15: *Simulation Results of Model (3.5.1) Showing the Disparity in Steady State Level of Replicated plus-strand RNA in VMS Caused by Changing Rate of Influx of HCV Plus-strand RNA from* $k_0 = 0$ *Represented by Dashed Blue Line, to* $k_0 = 2$ *Represented by Green Line, to* $k_0 = 8$ *Represented by Black Line, and to* $k_0 = 10$ *Represented by Thick Blue Line.*

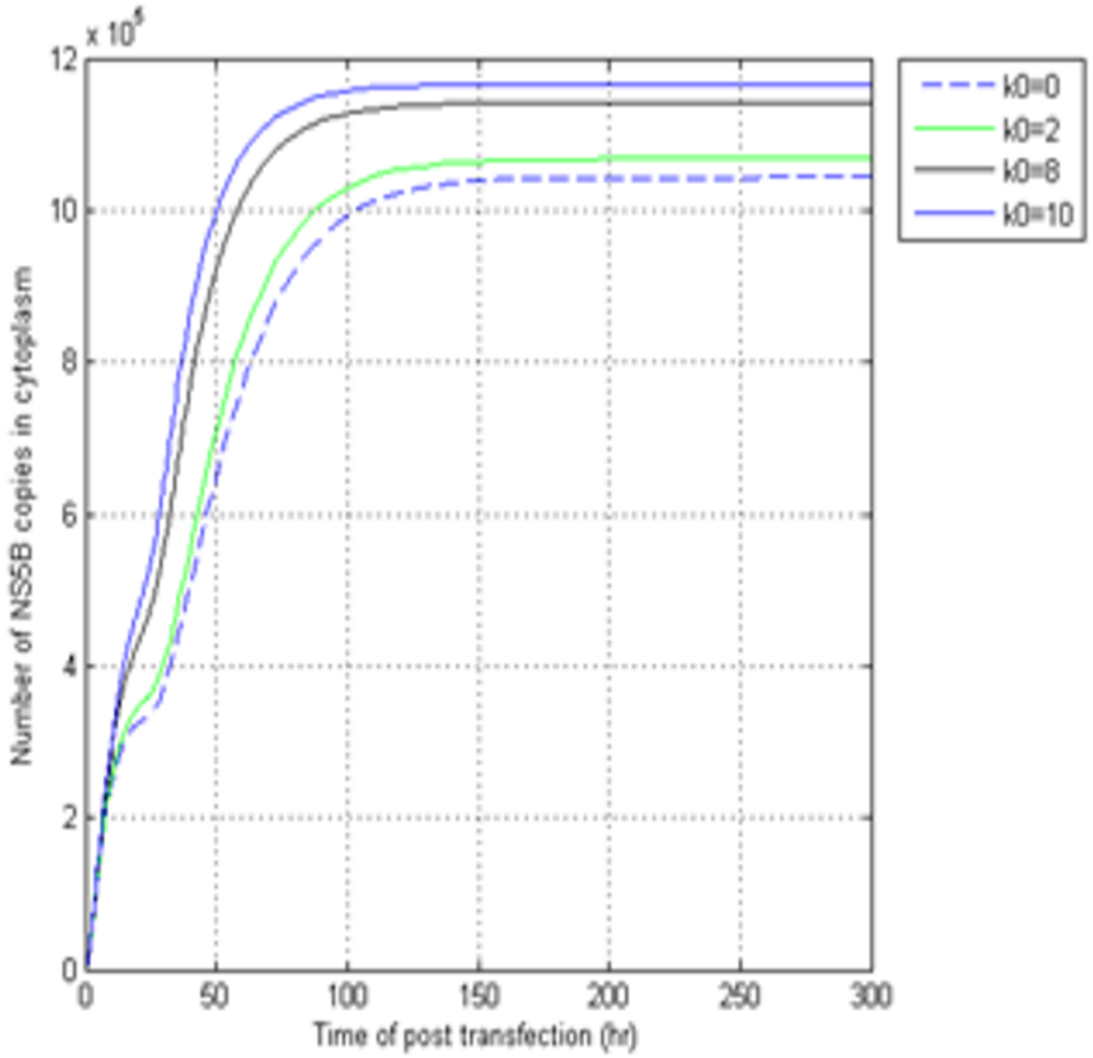

Figure 4.16: *Simulation Results of Model (3.5.1) Showing the Disparity in Steady State Level of NS5B (which is the key replication mechanism) Caused by Changing Rate of Influx of HCV Plus-strand RNA from* $k_0 = 0$ *Represented by Dashed Blue Line, to* $k_0 = 2$ *Represented by Green Line, to* $k_0 = 8$ *Represented by Black Line, and to* $k_0 = 10$ *Represented by Thick Blue Line.*

In figure (4.13-4.16), we observe the changes in steady state level of total plus-strand RNA, synthesized plus-strand RNA in the cytoplasm, replicated plus-strand RNA in VMS and NS5B respectively, as a result of changing rate of influx of HCV plus-strand RNA as shown in the following tables [Table 4.3 - Table 4.6].

Table 4.3: *Increase in Steady State Level of Total Plus-strand RNA in the System as a Result of Increase in* k_0.

Rate of Influx (k_0)	Steady state level of total plus-strand RNA
0	1380
2	1405
8	1590
10	5500

Table 4.4: *Increase in Steady State Level of Plus-strand RNA (synthesized) as a Result of Increase in* k_0.

Rate of Influx (k_0)	Steady state level of plus-strand RNA (synthesized)
0	11
2	14
8	60
10	2250

Table 4.5: *Increase in Steady State Level of Plus-strand RNA (replicated copies) as a Result of Increase in* k_0.

Rate of Influx (k_0)	Steady state level of plus-strand RNA (replicated copies)
0	590
2	610
8	680
10	2260

Figure 4.17 shows that the basic reproduction number increases as rate of influx of HCV plus-strand RNA increases. It was found that the healthy equilibrium is locally asymptotically stable when $R_0 < 1$ which is represented by solid line

Table 4.6: *Increase in Steady State Level of NS5B as a Result of Increase in* k_0.

Rate of Influx (k_0)	Steady state level of NS5B
0	10.3×10^5
2	10.4×10^5
8	10.7×10^5
10	10.8×10^5

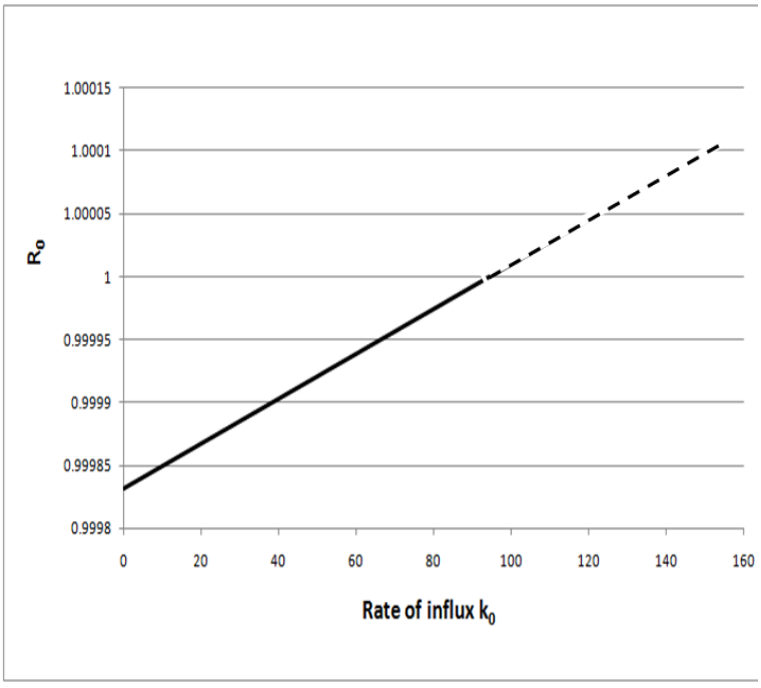

Figure 4.17: *Graph Showing Increase in* R_0 *Caused by Increase in Rate of Influx of HCV Plus-strand RNA*.

and unstable when $R_0 > 1$ represented by dashed line. It is also observed that the when rate of influx of HCV plus-strand RNA is less than 94 the healthy equilibrium is stable. It was also found that the endemic equilibrium exists when $R_0 > 1$ which is represented by the dashed line.

4.3 COMPARATIVE ANALYSIS

The modified model (3.5.1) corresponds to Dahari et al. [13] model, When rate of influx of HCV plus-strand RNA is zero. The modified model (3.5.1) shows that, when k_0 increases, then the steady state level of total plus-strand RNA in the system, synthesized plus-strand RNA in the cytoplasm, replicated copies of plus-strand RNA in VMS and NS5B also increase. While, Dahari et al. [13] found that k_{Ein} and μ_p^{cyp} are the parameters that most affect the steady state level of total plus-strand RNA in cell.

In Dahari et al. [13], number of ribosomes available for HCV translation is the only parameter that significantly affects the number of NS5B polymerase molecule in the cytoplasm, while in this research we found that rate of influx of HCV plus-strand RNA is another parameter that affects the number of NS5B polymerase molecule in the cytoplasm.

4.4 DISCUSSION

We have presented an extension of Dahari et al. model of subgenomic HCV replication in Huh-7 cell in [13] by incorporating the rate of influx of HCV plus-strand RNA (which is the viral particle) into the cell and monitor its effect in the system. It was found that changing the rate of influx of HCV plus-strand RNA also changes the steady state level of total plus-strand RNA in the system, synthesized plus-strand RNA in the cytoplasm, replicated plus-strand RNA in VMS, and NS5B (which is the key replication mechanism) respectively.

Three equilibria were identified, viz: the trivial equilibrium, the healthy equilibrium, and endemic equilibrium. Local stability of trivial equilibrium and healthy equilibrium were analyse. It was found that the trivial equilibrium could either be locally asymptotically stable or saddle point depending on certain threshold quantity.

Basic replication number was obtained and found that the healthy equilibrium E_1 is both locally and globally asymptotically stable when $R_0 < 1$. Further threshold analysis on R_0 reveals that, a high rate of influx of HCV plus-strand RNA can cause detrimental effect. It was also observed that R_0 is directly proportional to the rate of influx of HCV plus-strand RNA, that is when rate of influx of HCV plus-strand RNA increases, R_0 also increases and when rate of influx of HCV plus-strand RNA decreases, R_0 also decreases. Figure 4.17 verifies this statement.

CHAPTER FIVE

SUMMARY, CONCLUSION, AND RECOMMENDATIONS

5.1 INTRODUCTION

In this chapter, Section 5.2 gives the summary of this research work, while the conclusion and recommendations of the research are given in Section 5.3 and Section 5.4 respectively.

5.2 SUMMARY

This research work is a modification of Dahari et al. model in [13] model by incorporating the rate of influx of HCV plus-strand RNA with focus to investigate the intracellular dynamics, stability, and steady state of the system. We began by highlighting some of the biological insight of HCV infection.

The preliminaries of this research such as differential equation and concept of mathematical modelling were discussed briefly. Also we gave a review of HCV replication models including the Dahari et al. model in [13].

Complete HCV replication process was explained and then we derived the modified model from that explanation using reaction kinetics developed in section 3.2.

Three equilibrium points of the modified model were identified and the local stability of trivial and healthy equilibria were analysed. Condition for the existence of endemic equilibrium was obtained. The basic replication number of the modified model was obtained. We used a mathematical software MATLAB to simulate the model and tabulate a table showing how increase in rate of influx of HCV plus-strand RNA increased the number of replication mechanisms. The major findings of this research work were also discussed.

5.3 CONCLUSION

This research work is a modification of Dahari et al. (2007) model by incorporating rate of influx of HCV plus-strand RNA into Huh-7 cell. The following findings of the study are:

- Three equilibria were identified viz: trivial, healthy and arbitrary endemic equilibrium. Basic replication was obtained at healthy equilibrium which is directly proportional to the rate of influx of HCV plus-strand RNA.
- The study shows that the modified model is locally asymptotically stable when basic replicatin number is less than unity and unstable otherwise.
- The effects of rate of influx of HCV plus-strand RNA was assessed numerically by simulating the modified model with reasonable set of parameter values (mostly chosen from literature). The simulation reveals that:
  - At steady state, increasing rate of influx of HCV plus-strand RNA increases the number of molecules of: total plus-strand RNA in the cell,

plus-strand RNA (synthesized), plus-strand RNA (replicate copies), and NS5B polymerase.

- It was found that the rate of influx of HCV plus-strand RNA is another parameter that affects the number of NS5B polymerase molecule in the cytoplasm not as stated in [13] that number of ribosome available for HCV replication is the only parameter that affects the number of NS5B polymerase molecule in the cytoplasm.

Hence, from local stability analysis and simulation result, we can conclude that a serious intervention is required to reduce the rate of influx of HCV plus-strand RNA so as to control the replication of the virus.

5.4 RECOMMENDATIONS

The following are recommendations for further research:

1. This research work can be extended by including receptors (such as CD81, E2, lipoprotein, SI-BI, and so on) that play some role for the entry HCV RNA and study the effects of rate of influx of HCV plus-strand RNA.

2. A global stability analysis of the endemic equilibrium of the model is required.

3. A bifucation analysis of the model is also left for further research.

Bibliography

[1] Ashfaq U. A., Javed T., Rehman S., Nawaz Z., and Riazuddin S. An overview of hcv molecular biology, replication and immune response. *Virology J.*, 8:161, 2011.

[2] Chatterjee A., Guedj J., and Perelson A. S. Review mathematical modelling of hcv infection: what can it teach us in the era of direct-acting antiviral agents? *Antivaral Therapy*, 17:1171–1182, 2012.

[3] Wasley A. and Alter M. J. Epidemiology of hepatitis c: geographic differences and temporal trends. *Semin liver Dis.,*, 20(1):1–16, 2000.

[4] George L. M. Anna C. K., Arinze S. O. Huh-7 human liver cancer cells: A model system to understand hepatocellular carcinoma and therapy. *Journal of Cancer Therapy*, 4:606–631, 2013.

[5] Popescu C. and Dubuisson J. Role of lipid metabolism in hepatitis c virus assembly and entry. *Biol. Cell*, 102:63–74, 2010.

[6] Lavanchy D., Purcell R., Hollinger F. B., Howard C., Alberti A., Kew M., Dusheiko G., Alter M., Ayoola E., Beutels P., Bloomer R., Ferret B., Decker R., Esteban R., Fay O., Fields H., Fuller E. C., Grob P., Houghton M., Leung

N., Locarnini S. A., Margolis H., Meheus A., Miyamura T., Mohamed M. K., Tandon B., Thomas D., Head H. T., Toukan A. U., Van D. P., Zanetti A., Arthur R., Couper M., DAmelio R., Emmanuel J. C., Esteves K., Gavinio P., Griffiths E., Hallaj Z., Heuck C. C., Heymann D. L., Holck S. E., Kane M., Martinez L. J., Meslin F., Mochny I. S., Ndikuyeze A., Padilla A. M., Rodier G. M., Roure C., Savage F., and Vercauteren G. Global surveillance and control of hepatitis c. *Journal of Viral Hepatitis*, 6:35–47, 1999.

[7] Murray J. D. *Mathematical Biology:I. An Introduction*. Springer, 2002.

[8] Quinkert D., Bartenschlager R., and Lohmann V. Quantitative analysis of the hepatitis c virus replication complex. *Journal of Virology*, 79(21):13594–13605, 2005.

[9] Van den Driessche P. and James W. Reproduction numbers and sub-threshold endemic equilibria for compartmental models of disease transmission. *Mathematical Biosciences*, 180:2948, 2002.

[10] Burlone M. E. and Budkowska A. Hepatitis c virus entry: role of lopoprotein and cellular receptor. *J. of General Virology*, 90:1055–1070, 2009.

[11] Dahari H., Feliu A., Garcia-Retortillo M., Forns X., and Neumann A. U. Second hepatitis c replication compartment indicated by viral dynamics during liver transplantation. *J. Hepatol*, 42:491498, 2005.

[12] Dahari H., Feinstone S. M., and Major M. E. Meta-analysis of hepatitis c virus vaccine efficacy in chimpanzees indicates an importance for structural proteins. *Gastroenterology*, 139:965–974, 2010.

[13] Dahari H., Ruy M. R., Charles M. R., and Alan S. P. Mathematical modeling of subgenomic hepatitis c virus replication in huh-7 cells. *Journal of Virology*, 81:750–760, 2007.

[14] Hai-Feng H. and Na-Na S. Global stability for a binge drinking model with two stages. *Hindawi Publishing Corporation, Discrete Dynamics in Nature and Society*, Volume 2012:1–15, 2012.

[15] Ma H., Leveque V., Witte D. A., Li W., Hendricks T., Clausen S. M., Cammack N., and Klumpp K. Inhibition of native hepatitis c virus replicase by nucleotide and non-nucleoside inhibitors. *Virology*, 332:815, 2005.

[16] Dubuisson J., Helle F., and Cocquerel L. Early steps of the hepatitis c virus life cycle. *Cellular Microbiology*, 10(4):821–827, 2008.

[17] Biebricher C. K., Eigen M., and Luce R. Kinetic analysis of template-instructed and de novo rna synthesis by qβ replicase. *J. Mol. Biol.*, 148:391410, 1981.

[18] Michael K. and Gerhard D. *MATHEMATICAL MODELING: A Comprehensive Introduction*. Colorado State University, 2003.

[19] Choo Q. L., Kuo G., Weiner A. J., Overby L. R., Bradley D. W., and Houghton M. Isolation of a cdna clone derived from a bloodborne non-a, non-b viral hepatitis genome. *Science*, 244:359–362, 1989.

[20] Stuyver J. L., McBrayer R. T., Tharnish M. P., Hassan E. A., Chu K. C., Pankiewicz W. K., Watanabe A. K., Schinazi F. R., and Otto J. M. Dynamics of subgenomic hepatitis c virus replicon rna levels in huh-7 cells after

exposure to nucleoside antimetabolites. *Journal of Virology*, 77(19):10689–10694, 2003.

[21] Leela S. Lakshmikantham V. and Martynyuk A. A. *Stability Analysis of Nonlinear Systems*. Marcel Dekker, New York, Ny, USA, 1989.

[22] Andrew M., Ke C., Damien M., John E., and Zan L. *Evolution of Translation the Ribosome*. NIH Resource for Macromolecular Modeling and Bioinformatics, University of Illinois, 2011.

[23] Dorner M., Horwitz J. A., Robbins J. B., Barry W. T., Feng Q., Mu K., Jones C. T., Schoggins J. W., Catanese M. T., Burton D. R., Law M., Rice C. M., and Ploss A. A genetically humanized mouse model for hepatitis c virus infection. *Nature*, 474:208–211, 2011.

[24] Eigen M., Biebricher C. K., Gebinoga M., and Gardiner W. C. The hypercycle coupling of rna and protein biosynthesis in the infection cycle of an rna bacteriophage. *Biochemistry*, 30(46):1100511018, 1991.

[25] O'Connor C. M. and Adams J. U. *Essentials of Cell Biology*. Cambridge, MA: NPG Education, 2010.

[26] Yamuna M., Uday B., Adeesh N., and Himanshu P. Genetic code as binary bcd and gray code. *Research Journal of Pharmaceutical, Biological and Chemical Sciences*, 5(1):438, 2014.

[27] Ilya R. A. Pavel S. D. Vitaly A. L. Konstantin N. K. Dmitry I. T. Vitaly V. G. Maria G. S. Alexander M. S. Diana C. Lars K. Nikolay A. K. Vladimir A. I. Nikita V. I., Elena L. M. A new stochastic model for subgenomic hepatitis c

virus replication considers drug resistant mutants. *Plos One Journal*, 9(3):1–17, 2014.

[28] Department of health and human services. Hepatitis c general information. *Centers for Disease Control and Prevention, Division of Viral Hepatitis*, 21:1–2, 2010.

[29] Spiegelman P. Extracellular evolution of replicating molecules. *The neurosciences, Rockefeller university, New York*, In F. O. Schmitt (ed.):927, 1970.

[30] Bartenschlager R., Frase M., and Pietschmann T. Novel insights into hepatitis c virus replication and persistence. *Advances in virus research*, Academic press:71–180, 2004.

[31] Bartenschlager R. and Lohmann V. Replication of hepatitis c virus. *Journal of General Virology*, 81:16311648, 2000.

[32] Philippe R., Christophe H., Emmanuelle B., Denys B., and Malika A. Hepatitis c virus ultra-structure and morphogenesis. *Biology of the cell*, 96:103–108, 2004.

[33] Nurgary S. *Mathematical Modeling of Hepatitis C Virus Replication*. (unpublished doctoral thesis), Heidelberg University, Germany, June 2012.

[34] Lohmann V., Korner F., Koch J., Herian U., Theilmann L., and Bartenschlager R. Replication of subgenomic hepatitis c virus rna in a hepatoma cell line. *Science*, 285:110–113, 1999.

[35] Chu P. W. and Westaway E. G. Replication strategy of kunjin virus:evidence for recycling role of replicative form rna as template in semiconservative and asymmetric replication. *Virology*, 140:6879, 1985.

[36] Janak R. W. *Introduction to mathematical modelling*. University of Ruhuna, 2006.

APPENDIX

MATLAB CODE

```
function xprime =hepad(t,x)
xprime=zeros(9,1);
% Declaration of rate constants as used in literature
kc=0.6; kpin=0.2; kpout=0.2; kein=1.3e-5; k1=80; k2=100; k3=0.02; k4p=1.7;
k4m=1.7; k5=4; mip=0.04; me=0.04; mpc=10; mp=0.07; mds=0.06; mids=0.13;
mec=0.06; mtc=0.015; rbtot=700; k0=0;
% Evaluation of ribo
rb=rbtot-x(2);
% computation the differential equation
xprime(1)=k0*x(1)+k2*x(2)+kpout*x(5)-k1*rb*x(1)-kpin*x(1)-mpc*x(1);
xprime(2)=k1*rb*x(1)-k2*x(2)-mtc*x(2);
xprime(3)=k2*x(2)-kc*x(3);
xprime(4)=kc*x(3)-kein*x(4)-mec*x(4);
xprime(5)=-k3*x(5)*x(7)+k4p*x(9)+kpin*x(1)-(kpout+mp)*x(5);
xprime(6)=k4m*x(8)+k4p*x(9)-k5*x(6)*x(7)-mds*x(6);
xprime(7)=kein*x(4)+k4m*x(8)+k4p*x(9)-k3*x(5)*x(7)-k5*x(6)*x(7)-me*x(7);
xprime(8)=k3*x(5)*x(7)-k4m*x(8)-mip*x(8);
```

```
xprime(9)=k5*x(6)*x(7)-k4p*x(9)-mids*x(9);


    function xprime =hepad(t,x)
xprime=zeros(9,1);
% Declaration of rate constants as used in literature
kc=0.6; kpin=0.2; kpout=0.2; kein=1.3e-5; k1=80; k2=100; k3=0.02; k4p=1.7;
k4m=1.7; k5=4; mip=0.04; me=0.04; mpc=10; mp=0.07; mds=0.06; mids=0.13;
mec=0.06; mtc=0.015; rbtot=700; k0=2;
% Evaluation of ribo
rb=rbtot-x(2);
% computation the differential equation
xprime(1)=k0*x(1)+k2*x(2)+kpout*x(5)-k1*rb*x(1)-kpin*x(1)-mpc*x(1);
xprime(2)=k1*rb*x(1)-k2*x(2)-mtc*x(2);
xprime(3)=k2*x(2)-kc*x(3);
xprime(4)=kc*x(3)-kein*x(4)-mec*x(4);
xprime(5)=-k3*x(5)*x(7)+k4p*x(9)+kpin*x(1)-(kpout+mp)*x(5);
xprime(6)=k4m*x(8)+k4p*x(9)-k5*x(6)*x(7)-mds*x(6);
xprime(7)=kein*x(4)+k4m*x(8)+k4p*x(9)-k3*x(5)*x(7)-k5*x(6)*x(7)-me*x(7);
xprime(8)=k3*x(5)*x(7)-k4m*x(8)-mip*x(8);
xprime(9)=k5*x(6)*x(7)-k4p*x(9)-mids*x(9);


    function xprime =hepad(t,x)
xprime=zeros(9,1);
% Declaration of rate constants as used in literature
kc=0.6; kpin=0.2; kpout=0.2; kein=1.3e-5; k1=80; k2=100; k3=0.02; k4p=1.7;
```

```
k4m=1.7; k5=4; mip=0.04; me=0.04; mpc=10; mp=0.07; mds=0.06; mids=0.13;
mec=0.06; mtc=0.015; rbtot=700; k0=8;
% Evaluation of ribo
rb=rbtot-x(2);
% computation the differential equation
xprime(1)=k0*x(1)+k2*x(2)+kpout*x(5)-k1*rb*x(1)-kpin*x(1)-mpc*x(1);
xprime(2)=k1*rb*x(1)-k2*x(2)-mtc*x(2);
xprime(3)=k2*x(2)-kc*x(3);
xprime(4)=kc*x(3)-kein*x(4)-mec*x(4);
xprime(5)=-k3*x(5)*x(7)+k4p*x(9)+kpin*x(1)-(kpout+mp)*x(5);
xprime(6)=k4m*x(8)+k4p*x(9)-k5*x(6)*x(7)-mds*x(6);
xprime(7)=kein*x(4)+k4m*x(8)+k4p*x(9)-k3*x(5)*x(7)-k5*x(6)*x(7)-me*x(7);
xprime(8)=k3*x(5)*x(7)-k4m*x(8)-mip*x(8);
xprime(9)=k5*x(6)*x(7)-k4p*x(9)-mids*x(9);


    function xprime =hepad(t,x)
xprime=zeros(9,1);
% Declaration of rate constants as used in literature
kc=0.6; kpin=0.2; kpout=0.2; kein=1.3e-5; k1=80; k2=100; k3=0.02; k4p=1.7;
k4m=1.7; k5=4; mip=0.04; me=0.04; mpc=10; mp=0.07; mds=0.06; mids=0.13;
mec=0.06; mtc=0.015; rbtot=700; k0=10;
% Evaluation of ribo
rb=rbtot-x(2);
% computation the differential equation
xprime(1)=k0*x(1)+k2*x(2)+kpout*x(5)-k1*rb*x(1)-kpin*x(1)-mpc*x(1);
```

```
xprime(2)=k1*rb*x(1)-k2*x(2)-mtc*x(2);
xprime(3)=k2*x(2)-kc*x(3);
xprime(4)=kc*x(3)-kein*x(4)-mec*x(4);
xprime(5)=-k3*x(5)*x(7)+k4p*x(9)+kpin*x(1)-(kpout+mp)*x(5);
xprime(6)=k4m*x(8)+k4p*x(9)-k5*x(6)*x(7)-mds*x(6);
xprime(7)=kein*x(4)+k4m*x(8)+k4p*x(9)-k3*x(5)*x(7)-k5*x(6)*x(7)-me*x(7);
xprime(8)=k3*x(5)*x(7)-k4m*x(8)-mip*x(8);
xprime(9)=k5*x(6)*x(7)-k4p*x(9)-mids*x(9);

    y0=[500 0 0 0 0 0 0 0 0];
tspan=[0,300];
[T,Y]=ode15s(@hepad,tspan,y0);
[A,X]=ode15s(@hepad2,tspan,y0);
[B,Z]=ode15s(@hepad21,tspan,y0);
[C,P]=ode15s(@hepad22,tspan,y0);
xrptot=X(:,1);
rptot=Y(:,1);
zptot=Z(:,1);
pptot=P(:,1);
xrptot=X(:,5);
rptot=Y(:,5);
zptot=Z(:,5);
pptot=P(:,5);
xrptot=X(:,4);
rptot=Y(:,4);
```

zptot=Z(:,4);

pptot=P(:,4);

Total Plus-strand RNA in system ($R_p^c yp$)

plot(T,rptot,'–',A,xrptot,'g',B,zptot,'k',C,pptot,'b')

grid on

xlabel('Time of post transfection (hr)')

ylabel('Total plus strand RNA copies per cell')

Plus-strand RNA in cytoplasm (R_p)

grid on

xlabel('Time of post transfection (hr)')

ylabel('Number of replicated plus strand RNA')

NS5B

plot(T,rptot,'–',A,xrptot,'g',B,zptot,'k',C,pptot,'b')

grid on

xlabel('Time of post transfection (hr)')

ylabel('Number of NS5B copies in cytoplasm')